MASS TRANSFER AND BIOREMEDIATION OF PAHS IN A BEAD MILL BIOREACTOR

A Thesis

Submitted to the College of Graduate Studies and Research

In Partial Fulfilment of the Requirements

for the Degree of

Master of Science in the Department of Chemical Engineering

University of Saskatchewan

Saskatoon

By

Ryan Nathan Riess

Spring 2006

PERMISSION TO USE

In presenting this thesis in partial fulfillment of the requirements for a Postgraduate degree from the University of Saskatchewan, I agree that the libraries on campus may make it available for inspection. Further, I agree that permission for copying of this thesis in any manner, in whole or in part, for scholarly purposes may be granted by the professors who supervised my thesis work. In their absence the Head of the department of Chemical Engineering or the Dean of the College of Graduate Studies may give permission. It is understood that any copying or use of this thesis for financial gain shall not be allowed without my written permission. It is also understood that due recognition be given me and the University of Saskatchewan in any scholarly use which may be made of any material in my thesis.

Requests for permission to copy or to make other use of material in this thesis in whole or in part should be addressed to:

Head of the Department of Chemical Engineering

University of Saskatchewan

Saskatoon, Saskatchewan

Canada, S7N 5C9

ABSTRACT

Polycyclic aromatic hydrocarbons (PAH) have been identified as a serious environmental problem. In past research it has been proven that naphthalene, the simplest PAH, could be biodegraded using roller bioreactors and *Pseudomonas putida.* In this previous work it became apparent that the mass transfer rate of the hydrophobic naphthalene was the rate limiting factor in biodegradation, as the bacteria could degrade the naphthalene as fast as it entered solution. The challenge for the present research was to find a simple, inexpensive method for increasing the mass transfer rates within the framework of the previously successful reactor.

After some deliberation, the addition of inert particles (glass beads) was determined to be the preferred option to increase mass transfer. The inert particles visibly increased the turbulence in the reactor and significant increases in both mass transfer and bioremediation rates were achieved. The augmentation of mass transfer rates was found to be dependent on the type, size and relative loading of the particles. Two types of inert particles were investigated to increase mass transfer rates, spherical glass beads and Raschig rings. Glass beads were found to be far superior to Raschig rings for the intended purpose. Three sizes of spherical glass beads were then compared experimentally (1, 3, and 5mm). It was discovered that the 3mm beads were vastly superior to 1mm beads and 5 mm beads were slightly superior to 3mm beads. Different bead loadings (volume of particles / total working volume) were then explored with 10%, 25% and 50% bead loading investigated. Although

slight increases in mass transfer were observed at higher bead loadings, the reduction in working volume for biodegradation meant that 50% was accepted as the optimum loading parameter.

The optimum conditions for maximum mass transfer occurred using 5 mm spherical glass beads at 50% loading. The increase in mass transfer and biodegradation rates compared to a traditional roller bioreactor were found to be 10 fold and 11 fold, respectively. The optimum mass transfer conditions were then applied to 2-methylnaphthalene with increases in mass transfer and biodegradation equal to 6 fold and 8 fold, respectively. The candidate bacteria used in this study was found incapable of degrading 1,5 dimethylnaphthalene although the mass transfer results demonstrate promise for the developed technology. To determine the effects of scale on the process, two larger reactors were finally studied. They were eight times and twenty-one times the size of the initial bioreactor. The process was shown to speed up at larger scale which shows great promise for future applications. The maximum degradation rate achieved in the larger reactor was 148 $mgL^{-1}h^{-1}$. This compares very well with the best result found in literature, 119 $mgL^{-1}h^{-1}$, which was achieved in a much more complex system. Clearly, the bead mill bioreactor designed during the present work is a simple concept that shows superior performance for the bioremediation of PAH's.

ACKNOWLEDGEMENT

I would like to express my sincere gratitude to my co-supervisors, Drs. Gordon Hill and Mehdi Nemati. Their encouragement, guidance, and financial assistance were invaluable throughout this project.

I would also like to thank Environment Canada for financial assistance through the Science Horizons Youth Internship Program. In particular, thanks to Dr. John Headley for his support and encouragement in making the step of taking a master's degree.

Thank you to Dr. Richard Evitts and Dr. Catherine Nui for their hard work on my advisory committee and for the constructive criticism throughout this process. I would also like to thank Dr. Gordon Putz for being my external examiner.

Thanks to all the wonderful people in the Chemical Engineering Department. From the lab staff to the secretaries to my fellow grad students, everyone has been a pleasure to deal with.

DEDICATION

This thesis is dedicated to my family. Your belief in me and constant encouragement and support has made this project possible.

PERMISSION TO USE i
ABSTRACT ii
ACKNOWLEDGEMENTS iv
TABLE OF CONTENTS vi
LIST OF FIGURES ix
LIST OF TABLES xii
NOMENCLATURE xiv

CHAPTER 1 INTRODUCTION 1

1.1 Research Background 1

1.2 Research Objectives 4

1.3 Thesis Outline 5

CHAPTER 2 LITERATURE REVIEW 6

2.1 Polycylic Aromatic Hydrocarbons (PAHs) 6

2.1.1 Properties and Structure of PAHs 6

2.1.2 Sources and Fate of PAHs 9

2.1.3 Health concerns and toxicity of PAHs 11

2.2 Microbial Kinetics 12

2.3 Mass Transfer of PAHs 16

2.4 Bioremediation and Bioavailability of PAHs 18

2.5 Cometabolic Biodegradation 19

2.6 Bioreactors 21

2.6.1 Batch Reactor 21

2.6.2 Continuous Stirred Tank Reactor (CSTR) 22

2.6.3 Fed-batch Reactor (semi-batch) 24

2.6.4 Roller bioreactors 25

2.6.5 Bioreactor comparison 26

CHAPTER 3 THEORY 28

3.1 Mass Transfer 28

3.2 Bioremediation 31

CHAPTER 4 MATERIALS AND METHODS 35

4.1 Microorganisms, Medium and Chemicals 35

4.2 Experimental Apparatus 39

4.3 Procedures 43

4.3.1 Mass Transfer Experiments 43

4.3.2 Biodegradation Experiments 45

4.3.3 Biomass Concentration Measurements 46

4.3.4 Substrate Concentration Measurements 47

4.3.5 Toxicity Measurements 48

CHAPTER 5 RESULTS AND DISCUSSION 50

5.1 Mass Transfer Experiments 50

5.1.1 Effects of inert particle loading 50

5.1.2 Effects of Solid PAH concentration 53

5.1.3 Effects of Size and Type of Inert Particles 59

5.2 Biodegradation of Naphthalene 61

5.3 2-Methylnaphthalene Mass Transfer 63

5.4 2-Methylnaphthalene Biodegradation 64

5.5 1,5 Dimethylnaphthalene Mass Transfer 66

5.6 1,5 Dimethylnaphthalene Biodegradation 68

5.7 Cometabolization of Naphthalene and 2-Methylnaphthalene 68

5.8 Scale up Biodegradation Experiments 70

5.9 Bioremediation Products 74

5.10 Toxicity Results 76

CHAPTER 6 CONCLUSIONS AND RECOMMENDATIONS 77

6.1 Conclusions 77

6.2 Recommendations 79

REFERENCES 81

APPENDICES 86

Appendix A1: Calibration curve of biomass dry weight 86

Appendix A2: HPLC calibration curve for naphthalene 87

Appendix A3: HPLC calibration curve for 2-methylnaphthalene 88

Appendix A4: HPLC calibration curve for 1,5 dimethylnaphthalene 89

Appendix B: Experimental Data Tables 90

LIST OF FIGURES

Figure 2.1 The chemical structures of the most common PAHs (Sims and Overcash, 1983) **7**

Figure 2.2 The typical bacterial growth curve (Black, 1996) **12**

Figure 2.3: Schematic diagram of a batch reactor **22**

Figure 2.4: Schematic diagram of a CSTR **23**

Figure 2.5: Schematic diagram of fed-batch reactor **25**

Figure 3.1: Standard biodegradation curve (Purwaningsih et. al, 2004) **33**

Figure 3.2: Mass transfer limited degradation(Purwaningsih et. al, 2004) **34**

Figure 4.1 Mass transfer aids – from left to right: 3mm glass beads, Raschig rings, 5mm glass beads, 15mm marbles. **36**

Figure 4.2 Bellco roller apparatus **40**

Figure 4.3: Picture of the experimental setup – conventional reactor **41**

Figure 4.4: Reactor comparison left to right – bead mill bioreactor, 23 L reactor, 58 L reactor. **42**

Figure 4.5: Scale up roller apparatus used in the scale-up studies **43**

Figure 4.6: Optivisor 7X magnification headset **49**

Figure 5.1: Dissolution of 1000 mg/L particulate naphthalene at different loadings of glass beads **51**

Figure 5.2: Dissolution of 500 mg/L particulate naphthalene at different loadings of glass beads **53**

Figure 5.3: Dissolution of 5000 mg/L particulate naphthalene at different loadings of glass beads **54**

Figure 5.4: Dissolution of 10000 mg/L particulate naphthalene at different loadings of glass beads **55**

Figure 5.5: Calculation of k_La for 500mg/L naphthalene, 50% 5 mm beads. **56**

Figure 5.6: Dependency of volumetric mass transfer coefficient on concentration of particulate naphthalene and loading of glass beads **58**

Figure 5.7: Dissolution of 1000 mg/L of particulate naphthalene in the presence of Raschig rings and glass beads of different sizes (particle loading: 50%). **60**

Figure 5.8: Biodegradation of 500 mg/L of particulate naphthalene in conventional roller bioreactor (control) and in the bead mill bioreactors with 25 and 50% loadings of 5 mm glass beads **62**

Figure 5.9: Dissolution of 1000 mg/L particulate 2-methylnaphthalene in conventional roller bioreactor and bead mill bioreactor **63**

Figure 5.10: Biodegradation of 500 mg/L of particulate mono-methyl-naphthalene in the conventional roller bioreactor (control) and in the bead mill bioreactors **65**

Figure 5.11: Dissolution of 1000 mg particulate 1,5-dimethylnaphthalene in conventional roller bioreactor and bead mill bioreactor **67**

Figure 5.12: Biodegradation of 250mg/L naphthalene and 500 mg/L methylnaphthalene. **69**

Figure 5.13: Biodegradation in 20 L reactor (8 L working volume) **71**

Figure 5.14: Biodegradation in 58 L reactor (23 L working volume) **71**

Figure 5.16: HPLC chromatograms of the biodegradation progress. Top – initial reading, middle – intermediate reading, bottom – final reading. **75**

Figure A1: Calibration curve for biomass dry weight **86**

Figure A2: HPLC calibration curve for naphthalene **87**

Figure A3: HPLC calibration curve for 2-methylnaphthalene **88**

Figure A4: HPLC calibration curve for 1,5-dimethylnaphthalene **89**

LIST OF TABLES

Table 2.1 Physical and chemical properties of the most common PAHs (Sims and Overcash, 1983) **8**

Table 2.2 Industrial activities associated with production, processing, use, or disposal of PAH containing materials (Wilson and Jones, 1993) **10**

Table 2.3 Human activity effects on PAH concentration (Wilson and Jones, 1993) **11**

Table 4.1: Growth media minerals in 1 liter of distilled water **37**

Table 4.2: Trace element composition in 1 liter of distilled water **38**

Table 5.1: Naphthalene degradation rates reported in various studies **75**

Table 5.2: Toxicity data **78**

Table B1: Mass transfer comparison with 3mm beads in various loadings with solid naphthalene present at 1000mg/L **90**

Table B2: Mass transfer comparison with 3mm beads in various loadings with solid naphthalene present at 500 mg/L **90**

Table B3: Mass transfer comparison with 3mm beads in various loadings with solid naphthalene present at 5000 mg/L **90**

Table B4: Mass transfer comparison with 3mm beads in various loadings with solid naphthalene present at 10000 mg/L **91**

Table B5: Mass transfer comparison with various mass transfer aids at 50% loading. Naphthalene present at 1000mg/L **91**

Table B6: Biodegradation comparison of 3mm beads at various loadings with control. Initial naphthalene concentration 500mg/L **91**

Table B7: Biodegradation comparison of 5mm beads at various loadings with control. Initial naphthalene concentration 500mg/L **92**

Table B8: Mass transfer control data for 2-methylnaphthalene (1000mg/L) **92**

Table B9: Mass transfer optimum data for 2-methylnaphthalene. (50% loading 5mm glass beads, 1000mg/L) **92**

Table B10: Biodegradation and Cometabolization data for 2-methylnaphthalene at optimum mass transfer conditions **93**

Table B11: Mass transfer data for 1,5-dimethylnaphthalene at optimum mass transfer conditions and control **93**

Table B12: Scale-up biodegradation data for 20L reactor. Marbles occupied 50% of working volume **94**

Table B13: Scale-up biodegradation data for 53L reactor. Marbles occupied 50% of working volume. **94**

NOMENCLATURE

a	interfacial area in bioreactor (m^2m^{-3})
C_L	bulk PAH liquid concentration (mgL^{-1})
C_L*	saturation concentration of PAH adjacent to the solid (mgL^{-1})
C_S	solid (undissolved) PAH concentration (mgL^{-1})
C_T	PAH total concentration of both solid and aqueous phases (mgL^{-1})
D	diffusion coefficient (m^2h^{-1})
E	enzyme
ES	enzyme-substrate complex
EIS	enzyme-inhibitor-substrate complex
F	flow rate of new media into the reactor (Lh^{-1}).
K_I	inhibition constant (mgL^{-1})
k_L	mass transfer coefficient (mh^{-1})
k_La	overall volumetric mass transfer coefficient (h^{-1})
k_m	Michaelis-Menten constant (mgL^{-1})
Ks	saturation constant (mgL^{-1})
I	inhibitor concentration (mgL^{-1})
N	flux ($mgm^{-2}h^{-1}$)
P	product
r_s	rate of consumption of substrate ($mgL^{-1}h^{-1}$)
r_x	rate of biomass growth ($mgL^{-1}h^{-1}$)
S	substrate concentration (mgL^{-1})
S_F	substrate concentration found in the feed stream (mgL^{-1})
S_P	substrate concentration found in the product stream (mgL^{-1}),
t	time (s,h)
v	specific reaction rate (h^{-1})
v_{max}	maximum specific reaction rate (h^{-1})
V	volume of the media contained in the reactor (L)
X	biomass concentration (mgL^{-1})
Y_{XS}	cellular yield (mgL^{-1} biomass per mgL^{-1} substrate)

Greek letters

δ	film thickness (m)
μ	specific growth rate (h^{-1})
μ_{max}	maximum specific growth rate (h^{-1})

CHAPTER 1 INTRODUCTION

1.1 Research Background

Industrialization of the world has led to the production and subsequent release of a vast amount of harmful substances into the environment. The use and production of certain toxic compounds such as Chlorofluorocarbons (CFC's) have been curtailed but thousands of other substances continue to be produced and released. The Organization for Economic Co-operation and Development estimates that there are greater than 110 000 man-made chemicals still in commercial use, with hundreds being added to the list each year (OECD, 1999). Of major concern are those compounds which are both toxic and stable in the environment, a long-term lethal combination. These problematic compounds include many pesticides, polychlorinated hydrocarbons, organic solvents and polycyclic aromatic hydrocarbons (PAHs) (Chiou et al., 1998).

Industrial growth continues to be largely fuelled by fossil fuels, despite a plethora of recent advancements in alternative energy sources such as solar, wind and biomass. With industrialization increasing rapidly around the globe and a rapidly growing global population necessitating increasing reliance on fertilizers and pesticides, the amount of harmful chemicals entering the environment increases continually. Those chemicals may enter the environment through careless practice, intentional dumping or accidental release. Regardless of how they are released, these contaminants pose a huge challenge to the health and well being of the global population as a whole. A sustainable worldwide strategy is needed in order to deal with this growing global problem.

Canada is widely recognized as one of the most wealthy industrialized nations in the world. As such it has a responsibility to be environmentally progressive. In a few instances, Canada is in fact leading the way. Unfortunately in numerous other areas Canada is lagging far behind other industrialized nations. Recently, the Organization for Economic Cooperation and Diversification ranked Canada an appalling 28th out of 29 countries by using a list of twenty five environmental factors including: air, water, energy, biodiversity, waste, climate change, ozone depletion, agriculture, transportation and miscellaneous (*OECD,* 1999).

One of the ways in which Canada could improve upon its poor environmental track record is to make increasing use of novel bioremediation technologies. Bioremediation is a waste treatment approach utilizing biological processes. This includes the use of enzymes, bacteria, fungi, or plants to degrade, transform, sequester, mobilize, or contain contaminant organics, inorganics, or metallic pollutants (McMillen et al., 2001). Bioremediation can be used in soil, water or air. Bioremediation basically uses the metabolism of living organisms in order to break down harmful toxic substances into harmless or at least less harmful materials.

Microbial bioremediation is based on the fact that microorganisms need a source of carbon and energy to carry out basic life processes. Contaminants, which are often organic or inorganic compounds are able in many cases to provide that source of carbon and energy. Thus, selective increase of the favourable microorganisms population or enhancement of their metabolic activity

in the contaminated area can result in the bioremediation a contaminated area. Bioremediation can be highly effective and the costs associated with it are approximately ten times less than conventional remediation practices like incineration or extraction (OECD, 1999). In addition, bioremediation offers a final solution while land filling the waste in question or incinerating simply moves the contaminants to a different place. Bioremediation also restores the soil for possible further uses while conventional technologies permanently remove the soil in question from use.

Often, in nature, PAH contamination in soil is associated with free solid particles or as large particles sorbed directly on the soil, typically to the organic portion of the soil. Because biodegradation can only take place when particles are dissolved in the liquid phase, the biodegradation rate is limited by the dissolution rate of the solid particles. It is generally conceded that the majority of PAHs have extremely low rates of biodegradation in soil due to their low water solubility, high hydrophobicity and low bioavailability. Surfactants and water-miscible solvents have been used in the past to attempt to overcome these problems. These have largely failed because surfactants introduce an additional pollutant and the solubilization effects of cosolvents are generally insignificant for volume-fraction concentrations below 10% (Wang and Brusseau, 1993).

Biotechnologies for treatment of PAH contaminated sites can be characterized as either *in-situ* or *ex-situ* processes. *In-situ* bioremediation is typically very slow and difficult to control. *Ex-situ* treatment of contaminated soil or liquid streams in controlled bioreactors can be an extremely effective means of

transforming these harmful compounds into less harmful substances. Care must be taken however as PAHs are extremely volatile and susceptible to stripping losses (Gray et al.,1994). Previous studies have demonstrated that the dissolution rate of solid PAHs is the rate-limiting step in biodegradation (Volkering et al., 1993, Purwaningsih et al., 2004). Also clearly demonstrated in the past is that the hydrodynamic conditions inside the reactor greatly influenced the dissolution and biodegradation rate of the solid PAHs (Mulder et al., 1998).

This work is focused on overcoming the previously mentioned problems and improving biodegradation rates within the confines of a roller bioreactor. In this study, bioremediation of solid PAH particles was carried out in a slurry roller reactor under a variety of hydrodynamic conditions. The reactor was entirely enclosed to prevent volitilization and stripping losses. Prior to bioremediation experiments, a rigourous investigation on the extent of mass transfer was undertaken for each of the hydrodynamic conditions used. In this manner, a set of conditions which optimize mass transfer and thus bioremediation was discovered and subsequently applied in all subsequent bioremediation experiments.

1.2 Research Objectives

The objectives of this research were:

1) To study the mass transfer characteristics of a number of polycyclic aromatic hydrocarbons in a roller bioreactor and find simple and economical strategies to increase the rates of mass transfer, through modification of the bioreactor design.

2) To assess the effects of bioreactor design (improved mass transfer) on the extent and the rate of biodegradation for a variety of polycyclic aromatic hydrocarbons
3) To study the impact of scale-up on the performance of the developed bioreactor.

1.3 Thesis Outline

This thesis is arranged into six chapters. Chapter one gives an introduction to the research and the scope and objectives of this thesis. Chapter two encompasses a literature review which covers previous work and developments in the area of PAH bioremediation and the challenges inherent to dealing with volatile hydrophobic substances. The theory involved in this work is presented in Chapter three including the relevant mass transfer considerations and bioremediation theory. Chapter four focuses on the experimental work. It details the microorganism, medium and chemicals utilized, the experimental setup, the experimental procedures and analytical methods and instruments used in this study. Chapter five describes the experimental results, data analysis and discussion. Finally, Chapter six highlights the important findings of the present work and makes several recommendations for future studies.

CHAPTER 2 LITERATURE REVIEW

2.1 Polycyclic Aromatic Hydrocarbons (PAHs)

2.1.1 Properties and Structure of PAHs

PAHs constitute a diverse class of organic compounds consisting of two or more benzene rings fused in linear, angular or cluster orientations (Prabhu and Phale, 2003). The physical properties and chemical structures of the most common PAHs are presented in Figure 2.1 and Table 2.1 respectively. The physical properties of PAHs vary with their molecular weight and structure. PAHs have low to extremely low water solubility and also moderate to low vapour pressures. As a general rule, the hydrophobicity increases and the aqueous solubility decreases with an increase in the number of aromatic rings (Wilson and Jones, 1993). The PAHs octanol-water coefficients (K_{ow}) are quite high which indicates a great potential for adsorption to suspended particulates in air or water as opposed to vapour or dissolved phases. PAHs consist of a large variety of structures ranging from two fused benzene rings all the way up to more than six arranged in various orientations. They may also be methylated to various degrees. In general, the more methyl groups a PAH contains, the lower its solubility will be.

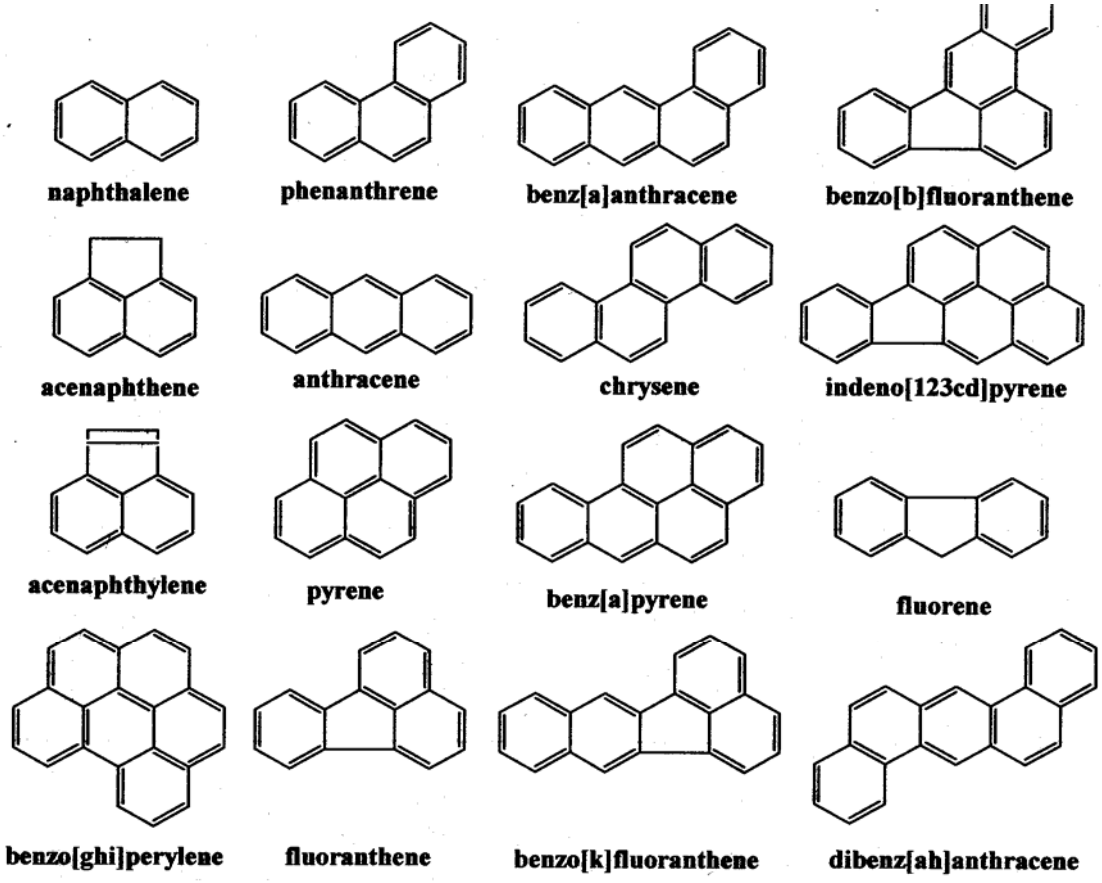

Figure 2.1 The chemical structures of the most common PAHs (Sims and Overcash, 1983)

Table 2.1 Physical and chemical properties of the most common PAHs (Sims and Overcash, 1983).

PAH	Molecular weight	Aqueous solubility at 30° C [mg L^{-1}]	Vapour pressure / [N m^{-2} at 20°C]	Log octanol/ water partition coefficient
naphthalene	128	31.7	6.56	3.37
acenaphthylene	152	3.93	3.87	4.07
acenapthene	154	3.47	2.67	4.33
fluorene	166	1.98	1.73	4.18
phenanthrene	178	1.29	$9.07*10^{-2}$	4.46
anthracene	178	$7.30*10^{-2}$	$2.61*10^{-2}$	4.45
pyrene	202	$1.35*10^{-1}$	$8.00*10^{-4}$	5.32
fluoranthene	202	$2.60*10^{-1}$	$9.11*10^{-5}$	5.33
benz[a]anthracene	228	$4.00*10^{-2}$	$6.67*10^{-7}$	5.61
chrysene	228	$2.00*10^{-3}$	$8.40*10^{-5}$	5.61
benz[a]pyrene	252	$4.00*10^{-3}$	$6.67*10^{-5}$	6.04
benzo[k]fluoranthene	252	$1.20*10^{-3}$	$6.67*10^{-5}$	6.57
benzo[b]fluoranthene	252	$5.50*10^{-4}$	$6.67*10^{-5}$	6.84
indeno[123cd]pyrene	276	$6.20*10^{-2}$	$1.33*10^{-8}$	7.66
benzo[ghi]perylene	276	$2.60*10^{-4}$	$1.33*10^{-8}$	7.23
dibenz[ah]anthracene	276	$5.00*10^{-4}$	$1.33*10^{-8}$	5.97

2.1.2 Sources and Fate of PAHs

Industrial activities and agricultural developments release a vast amount of hazardous compounds into the environment. Polycyclic aromatic hydrocarbons (PAHs) of natural and anthropogenic origins form a major portion of these contaminants (da Silva et al., 2003). PAHs result naturally from such events as volcanic eruptions, the burning of organic matter, and the decay of organic matter. Forest fires in Canada result in the release of approximately 2000 tonnes (t) of PAHs each year which constitutes 50% of the total recorded atmospheric release inventoried (CEPA, 1994). PAHs are widely distributed in the environment, particularly in industrial sites associated with petroleum and gas processing (Langworthy et al., 2002). They are natural constituents of fossil fuels and are commonly formed during incomplete combustion of organic material. PAHs are thus present in large concentrations in the products of the refining of fossil fuels (Wang et al., 1990). The refining and transport of petroleum products is a major contributor of localized loadings of PAHs in the environment. These loadings can occur through accidental spills of the refined or raw products and through the discharge of industrial effluents (Kanaly and Haryama, 2000). PAHs are released from the combustion of gasoline or diesel fuel and from cigarette smoke, among other very common sources (Marr et al., 1999). Table 2.2 provides a list of common sources of PAHs. As a result of this universal distribution, PAHs are found in air, in soils and sediments, in surface water and in groundwater. The need to develop practical and effective bioremediation strategies for PAHs is a global priority.

Table 2.2 Industrial activities associated with production, processing, use, or disposal of PAH containing materials (Wilson and Jones, 1993)

Gasification/liquefaction of fossil fuels
Heat and power generation by using fossil fuels
Coke production
Catalytic cracking
Carbon-black production and use
Asphalt production and use
Coal-tar pitch production and use
Refining/distillation of crude oil and derived products
Wood-treatment processes
Wood-preservation production
Fuel/oil storage, transportation, processing, use and disposal
Landfill/waste dumps
Open burning (tires/coal etc.)
Incineration

Upon release, the atmosphere provides the primary means of transport for PAHs. PAHs readily adsorb on particulates in the atmosphere and can be carried long distances before being secured in soil or water through surface run-off. Due to their hydrophobicity, PAHs readily build up in sediments and partition to other organic particles in soil or water. The structural characteristics of PAHs such as number of rings, angularity, as well as their low solubility and high hydrophobicity make them persistent in the environment (Sutherland, 1992). Human activity has a huge impact on PAH levels in the environment. Table 2.3 gives an idea of the extent human activity has on background PAH concentrations

Table 2.3 Human activity effects on PAH concentration (Wilson and Jones, 1993)

Compound	Concentrations (µg/kg)		
	Rural soil	Agricultural Soil	Urban Soil
Acenaphthene	1.7	6	
Acenaphthylene		5	
Anthracene		11–13	
Benzo(a)anthracene	5–20	56–110	169–59,000
Benzo(a)pyrene	2–1,300	4.6–900	165–220
Benzo(b)fluoranthene	20–30	58–220	15,000–62,000
Benzo(e)pyrene		53–130	60–14,000
Benzo(g,h,i)perylene	10–70	66	900–47,000
Benzo(k)fluoranthene	10–110	58–250	300–26,000
Chrysene	38.3	78–120	251–640
Fluoranthene	0.3–40	120–210	200–166,000
Fluorene		9.7	
Ideno(1,2,3-c,d)pyrene	10–15	63–100	8,000–61,000
Phenanthrene	30.0	48–140	
Pyrene	1–19.7	99–150	145–147,000

2.1.3 Health concerns and toxicity of PAHs

PAHs in general are becoming an increasing risk to the overall health of the environment from the bottom of the food chain to the top. Because of their lipophilic nature, PAHs pose a large threat of biomagnification through trophic transfers (Twiss et al., 1999). PAHs are also widely known to produce acute toxic effects as well as mutagenic and/or carcinogenic effects (Phillips, 1983).

Humans are exposed to PAHs through contaminated air, soil and the food chain. The first reported instance of PAH toxicity occurred in 1932 when Taylor and Russell reported that naphthalene poisoning resulted in anaemia. Naphthalene toxicity has since been linked to various other disorders (Wilson et al, 1996) and

an abnormally high rate of laryngeal tumours is reported among young children of workers in PAH chemical industries (Perera et al., 2002).

2.2 Microbial Kinetics

In a batch system, a typical bacterial growth curve includes four phases: lag phase, exponential growth phase, stationary phase and finally death phase. The lag phase begins with inoculation of the system with bacteria. In this phase the bacteria are becoming acclimated to their new environment and are not actively dividing. The size of the inoculum, as well as the type of carbon source used for the growth and maintenance of culture used as the inoculum affects the length of the lag phase. If the inoculum was grown on the same carbon source being used in the reactor, the lag phase will be significantly shorter as the bacteria are already equipped to break down that carbon source. If there are multiple carbon sources present, multiple lag phases may be observed. This is caused by a shift in the metabolic pathway within a growth cycle. Figure 2.2 provides a graphical interpretation of a typical bacterial growth cycle in a batch system.

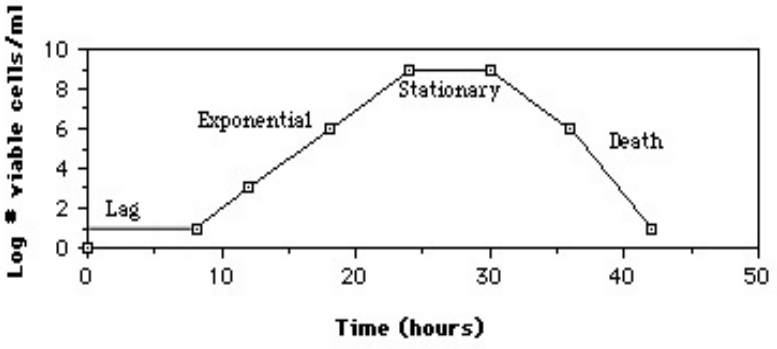

Figure 2.2 The typical bacterial growth curve (Black, 1996)

The exponential phase is also known as the logarithmic growth phase. This phase occurs once the bacteria are acclimated to the new surroundings and growth occurs rapidly by binary fission. Growth depends on the specific growth rate and biomass concentration. This is best described mathematically by:

$$\frac{dX}{dt} = \mu X \tag{2.1}$$

This equation defines the specific growth rate μ and the biomass concentration, *X*. If the specific growth rate is constant, the growth of biomass is then exponential. This can only occur if μ is independent of substrate concentration, S and biomass concentration.

Exponential growth cannot be sustained indefinitely in a batch system. Eventually, growth is slowed by one of three factors: lack of nutrients, build up of inhibitory metabolites or end products, or exhaustion of biological space. During the stationary phase, it is impossible to tell if equal numbers of cells are dividing as are dying or if the population has simply ceased growing and dividing. Secondary metabolites, such as antibiotics, are produced during the stationary phase.

If the system is left undisturbed, a death phase follows the stationary phase. The population declines rapidly in this stage and is essentially the reverse of the exponential growth stage. Cells are no longer dividing and are dying at a constant rate.

Microbial kinetics are much more complex than they first appear. At the basic level, they use a specific substance as substrate and produce certain end products including more biomass. A closer look reveals that there are many

complex reactions occurring inside microorganisms. These complex reactions are controlled by enzymes, which are protein catalysts. They are incredibly effective in promoting specific biochemical reactions. The substrate (*S*) reacts with an enzyme (*E*) to form an enzyme-substrate complex (*ES*) which eventually reacts to form the product (*P*) and the free enzyme according to the following reactions:

$$E + S \leftrightarrow ES \tag{2.2}$$

$$ES \rightarrow P + E \tag{2.3}$$

Michaelis and Menten developed a fundamental relationship for a reaction catalyzed by a single enzyme (Bailey and Ollis, 1977):

$$v = \frac{v_{\max} S}{k_m + S} \tag{2.4}$$

where v is the specific reaction rate ($mgL^{-1}s^{-1}$), v_{max} is maximum reaction rate ($mgL^{-1}s^{-1}$), and k_m is the Michaelis-Menten constant (mgL^{-1}).

In 1942, it was proposed that a single enzyme reaction likely controlled the growth of the cell (Monod, 1942). If this single reaction follows the form of Michaelis-Menten, Monod found:

$$\frac{dX}{dt} = \frac{\mu_m S X}{K_s + S} \tag{2.5}$$

where μ_m is the maximum specific growth rate (s^{-1}) and K_S (mgL^{-1}) is the saturation constant. Most commonly encountered growth situations fit the Monod model well.

In many cases reactions catalyzed by enzymes are inhibited by certain molecules which lower the rate of the reaction. There are three different types of inhibition: competitive, non-competitive and uncompetitive. Inhibition is a way in which cells can control the rate of enzymatic reactions. Inhibition mechanisms usually operate by having the inhibitor bind to the enzyme, thus blocking the substrate from being utilized. *EIS* stands for the inhibited complex.

$$E + S \Leftrightarrow ES \Rightarrow P + E \tag{2.6}$$

$$ES + I \Leftrightarrow EIS \tag{2.7}$$

The reaction rate relationship for inhibited enzyme catalysed reactions is derived from equation 2.4 (Bailey and Ollis, 1977):

$$v = \frac{v_{\max} S}{k_m + S + \frac{SI}{K_I}} \tag{2.8}$$

where K_I is the inhibition constant (mgL^{-1}) and I is the concentration of the inhibitor (mgL^{-1}). At times, the growth inhibiting substance is the substrate itself. This is referred to as substrate inhibited growth. Substrate inhibited growth occurs most frequently when microorganisms use a toxic compound as their main carbon source. A kinetic growth model for substrate inhibited growth was proposed by Haldane in 1930 (Haldane, 1930) and is based on the relationship presented in Equation 2.7. By setting the inhibitory substance $I = S$, he derived:

$$\frac{dX}{dt} = \frac{\mu_m SX}{K_s + S + S^2 / K_I} \tag{2.9}$$

Finally, the yield of biomass per unit of substrate consumed is an important parameter when dealing with microbial growth. This quantity is commonly known as cellular yield, Y_{XS} and is given by:

$$\frac{dS}{dt} = -\left(\frac{dX}{dt}\right)\frac{1}{Y_{XS}} \tag{2.10}$$

2.3 Mass Transfer of PAHs

It is abundantly clear that the vast majority of microbial uptake of PAHs occurs in the aqueous phase (Volkering et al., 1992). Biodegradation of PAHs in the solid state is next to impossible and only occurs after the dissolution of these organic molecules in water. The mass transfer or dissolution of solid particles in a liquid is a much studied topic. Basically, molecules which are on the surface of the particle leave continuously into the liquid phase at the expense of the solid phase. This transfer is made up of two key steps. First is the transfer of the molecules from the solid surface to the liquid film surrounding the particle. From there, the molecules diffuse into the bulk liquid phase. The rate molecules of dissolution can be described by using a term known as the solid-liquid lumped mass transfer coefficient. This term is derived in Chapter Three.

One factor that has a large impact on mass transfer rates is the hydrodynamic conditions within the system. Because the solubility of PAHs is very low, the amount of resistance to mass transfer into the liquid phase can be of primary importance. Mulder et al., (1998) clearly showed that an increase in

the mass transfer coefficient for naphthalene was correlated with an increase in the impeller speed in the bioreactor. They determined that increases in agitation speed create the turbulence at the solid-liquid interface, thereby reducing the film thickness and enhancing the mass transfer coefficient.

Organic chemicals possess a characteristic affinity to vaporize from either the solid or liquid state (Singh and Hill, 1987). Once steady state is attained, this affinity results in an equilibrium concentration of airborne organic molecules in the atmosphere immediately in contact with the chemical. This condition is maintained by molecules condensing as quickly into the liquid or solid state as other molecules are vaporizing to replace them. PAH's with three or more rings are considered semi-volatile organic contaminants (Thomas, 1982). They have Henry's coefficients (H) in the range of $10^{-5} < H < 10^{-3}$ atm-$m^3$$mol^{-1}$. Within this range of H, volatilization is not considered rapid. Conversely, naphthalene with two rings is considered to be a volatile compound. In an earlier air stripping study, (Labranche and Collins, 1996) it was demonstrated that the highest rate of mass transfer of organic compounds to air is achieved when the Henry's coefficient is high and the solubility in water is very low. Because smaller PAHs have a high Henry's coefficient, there is a greater chance of losing substrate due to air stripping. This loss is highly undesirable as it slows bacteria growth and gives false results. The concentration of substrate in the liquid may drop dramatically, but it has just been transferred to the gas phase (Labranche and Collins, 1996). This is highly undesirable and must be avoided in any remediation strategy.

2.4 Bioremediation and Bioavailability of PAHs

The majority of organic chemicals can be utilized as a carbon source for living organisms (yeast, fungi, or bacteria). The organisms rely on specialized enzymes to carry out the breakdown of these chemicals and this destruction of chemicals is known as biodegradation. The intentional use of the process of biodegradation for productive purposes is known as bioremediation. The goal of bioremediation is to break down hazardous or toxic organic pollutants into harmless by products like carbon dioxide, water and cell proteins.

The commonly accepted definition of bioavailability is the amount of contaminant present that can be readily taken up by microorganisms and subsequently degraded (Maier, 2000). Bioavailability is the controlling step in biodegradation, because if there is not enough of a carbon source available to the living organisms, the organisms will not multiply and make use of the contaminant. There are several conditions required in order for biodegradation to occur in the environment. These conditions are identified as (Alexander 1999):

1) An organism must exist which has the necessary enzymes to achieve the biodegradation.
2) That specific organism must be present within the vicinity containing the chemical.
3) If the enzymes catalyzing the initial step of degradation are intracellular, the molecule must first pass through the cell membrane to the internal location where the enzyme is to act.

4) Because the initial population of biomass (fungi or bacteria) acting on organic compounds is initially very small, the environmental conditions must be favourable in order to allow for the proliferation of potentially active microorganisms.

Bioremediation may occur under either aerobic or anaerobic conditions. Bioremediation is more common under aerobic conditions during which microorganisms make use of atmospheric oxygen as an oxidizing agent in order to carry out the degradation of organics which are generally in a very low oxidation state. Under anaerobic conditions, biological activity is carried out in the absence of oxygen and other molecules such as nitrates must be used as oxidizing agents. Anaerobic biological activity is generally much slower than aerobic biological activity. In either case, during the degradation of the original contaminants, intermediate products which are more, less, or in some cases equally as toxic as the original contaminants may be created (Alexander, 1999).

2.5 Cometabolic Degradation

The majority of organic compounds found in nature are easily degraded by microorganisms. Polyaromatics are resistant to biological attack and are often toxic to living cells (Alexander, 1999). In Nature, it is exceedingly rare to find single species of organic compounds in a given area. Organics are almost exclusively found in mixtures. Given this fact, it is important to understand the growth behaviour of single microbial species on mixtures of organic compounds (Hill et al., 1996). The term cometabolization is defined as transformation of a non-growth substrate by growing cells in the presence of a growth substrate, by

resting cells in the absence of a growth substrate, or by resting cells in the presence of an energy substrate (Horvarth, 1972). A growth substrate is defined as a donor of electrons that provides energy required for cell growth and maintenance, while an energy substrate is defined as an electron donor that provides energy, but does not support growth by itself.

Several reasons for cometabolization have been proposed including: (Alexander, 1999)

1) The initial substrate is transformed to products that inhibit the activity of late enzymes in mineralization or that suppress growth of the organism.

2) The initial enzyme or enzymes convert substrate to an organic product that is not further transformed by other enzymes in the microorganism to yield the metabolic intermediates that ultimately are used for biosynthesis and energy production.

3) The organism needs a second substrate to bring about some crucial metabolic reaction.

The use of non-toxic, easily biodegradable organic compounds to enhance the degradation of toxic pollutants by cometabolization has attracted a host of research interest (Tarighian, 1999) Varying degrees of success has been achieved in the enhancement of biodegradation rates, but the area warrants further study.

2.6 Bioreactors

At the core of all biochemical processing is the bioreactor. The bioreactor is a vessel which contains materials to be treated using either bacteria or enzymes. For any given process, the bioreactor should be carefully designed to ensure that it is appropriate for the given task. By combining knowledge of material and energy balances with an understanding of bacterial kinetics, a suitable bioreactor can be optimized for a given transformation. For industrial concerns, the quality of the final desired product is extremely important. Cost is a huge issue as well. The bioreactor should be designed in such a way as to minimize costs while still retaining the desired treatment quality (Van't Riet and Trampe, 1991).

The equations used to quantify performance for bioreactors are derived under steady state conditions and assume constant temperature and constant liquid density. These conditions are reasonably common for most biochemical processes. A simple material balance base on the reactants or products over the bioreactor is developed based on the simple governing equation based on conservation of mass:

Accumulation Rate = Input Rate – Output Rate + Production Rate (2.10)

2.6.1 Batch Reactor

Bioreactors come in a variety of shapes and basic designs. The most basic type is the batch reactor (Figure 2.3). Its primary characteristic is that there is neither inflow nor outflow into the system while the reaction is proceeding. The desired cells are cultured and are added at the start to the mixture to be treated.

Steady mixing is maintained in order to ensure a homogeneous composition in all areas of the reactor. Once the given process is completed, the bioreactor contents are then discharged. The performance equation from the material balance for the substrate becomes:

$$r_s = \left(\frac{dS}{dt}\right) = -\mu \frac{X}{Y_{XS}} \tag{2.11}$$

in the above equation t is the time (s) and r_s is the rate of consumption of substrate ($mgL^{-1}s^{-1}$).

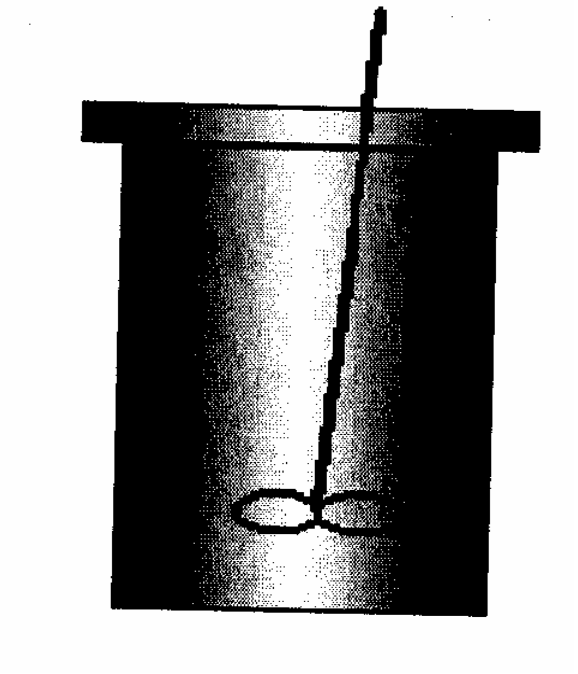

Figure 2.3: Schematic diagram of a batch reactor

2.6.2 Continuous Stirred Tank Reactor (CSTR)

A slightly more complicated bioreactor is the continuous stirred tank reactor (CSTR, Figure 2.4) It differs from a batch reactor in that reactants are continuously fed into the reactor and products are continually removed. Mixing is

achieved by using an impeller or else by sparging with air. The performance equation for a CSTR is obtained from the steady state material balance and yields for the substrate:

$$\frac{V}{F} = \frac{S_F - S_P}{r_s} \qquad (2.12)$$

where S_F is simply the substrate concentration found in the feed stream (mgL^{-1}),, S_P is the substrate concentration found in the product stream (mgL^{-1}), V is the volume of the media contained in the reactor (constant at steady state, L) and F is the flow rate of new media into the reactor (Ls^{-1}).

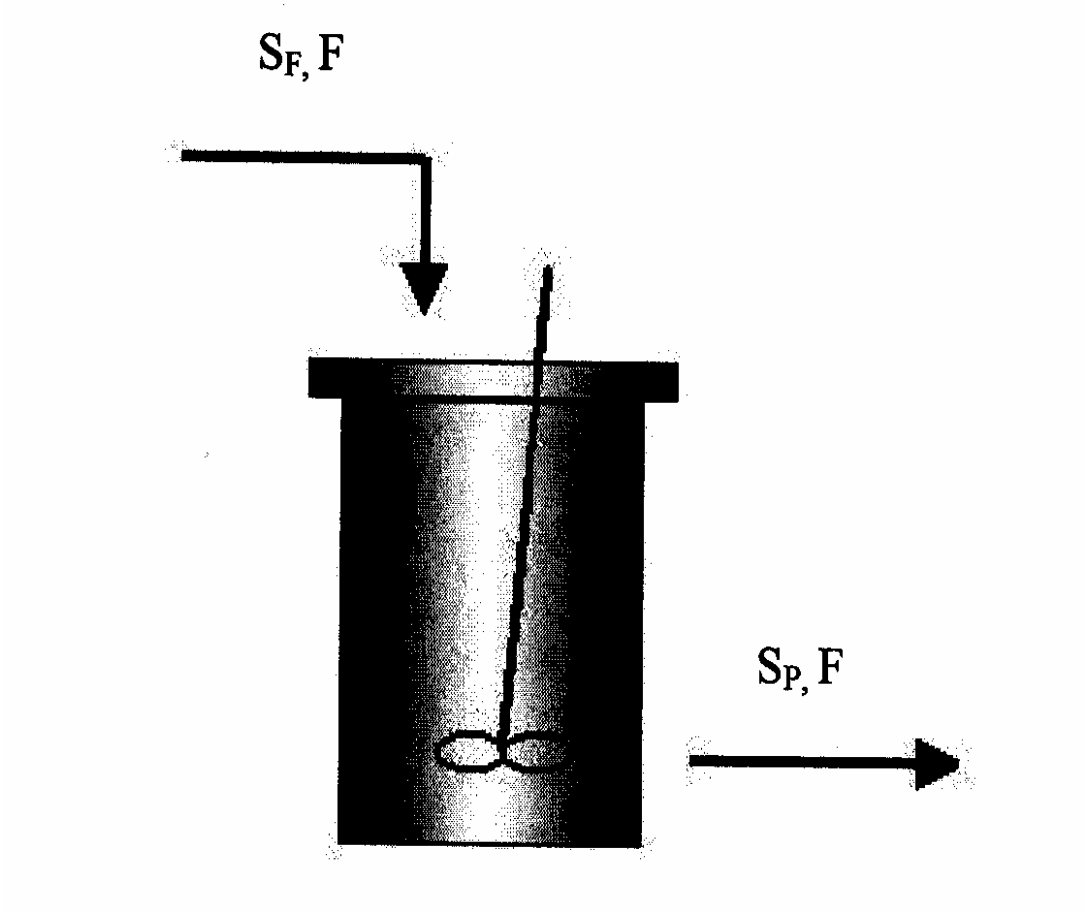

Figure 2.4: Schematic diagram of a CSTR

2.6.3 Fed-batch Reactor (semi-batch)

A third type of bioreactor combines elements of both batch and CSTR reactors. It is known as either a Fed-batch Reactor or a semi-batch reactor (Figure 2.5). In a fed-batch reactor, nutrients are added continuously or periodically, and the reactor content is removed periodically. The advantages of the fed-batch reactor are an ability to overcome substrate inhibition and overflow metabolism or to ensure nutrient and oxygen sufficiency with well planned intermittent feeding of substrate and nutrients to the reactor. From the material balance over the reactor, the equations commonly used for semi-batch reactors for biomass and substrate are as follows:

$$\frac{dX}{dt} = r_x - \left(\frac{FX}{V}\right) \tag{2.13}$$

$$\frac{dS}{dt} = \left(\frac{F\left(S_F - S_P\right)}{V}\right) - r_s \tag{2.14}$$

where r_x is the rate of biomass growth ($mgL^{-1}s^{-1}$) and r_s is the rate of substrate depletion ($mgL^{-1}s^{-1}$).

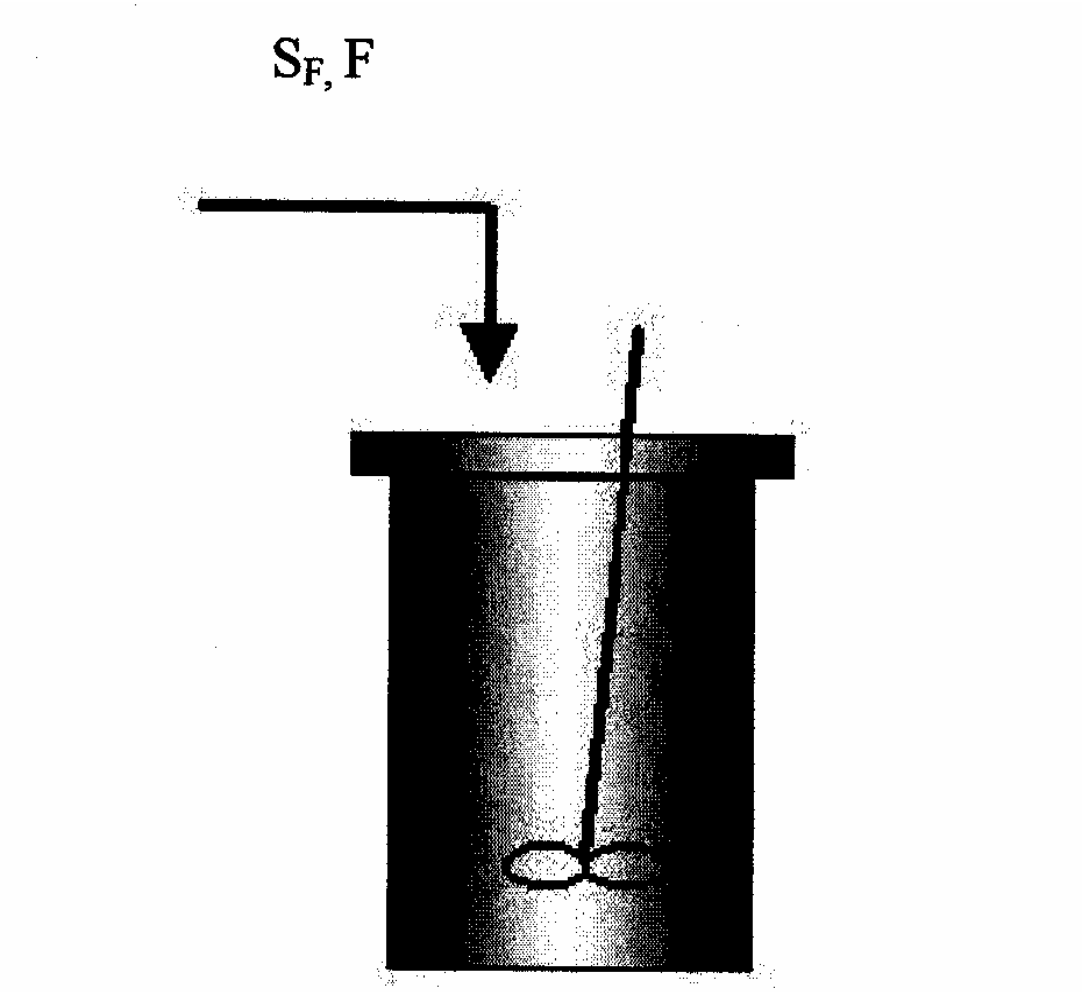

Figure 2.5: Schematic diagram of fed-batch reactor

2.6.4 Roller Bioreactors

Roller bioreactors are a fourth type of reactor that is not as common as the other three. In brief, a roller bioreactor consists of a sealed container in which mixing is achieved as a result of continuous rotation of the reactor on rollers. There are several benefits offered by a roller bioreactor over the other types of reactors. This includes that there is no mechanical stirring, which can transport particles out of solution. Most conventional reactors have properties which allow hydrophobic particles to cling to surfaces which results in low bioavailability.

The roller bioreactor neither offers surfaces for hydrophobic particles to cling to nor creates detrimental shear forces to damage cell walls.

The roller bioreactor used for the purposes of this study was operated much like a batch reactor. Instead of using an impeller to mix the solution, the reactor is simply rotated at a given controlled speed. Air can be supplied as needed by inserting a sparger tube through a central axial opening in the reactor.

2.6.5 Bioreactor Comparison

One of the main barriers to successful bioremediation of PAHs is the hydrophobicity and low solubility of these compounds in the aqueous phase, resulting in significant mass transfer limitations within the bioreactor (Mulder et al., 1998). In the majority of bioreactors, mass transfer becomes the limiting factor in degradation. The bacteria are able to break down the PAHs as fast as they enter the liquid phase. Stirred tank bioreactors offer an advantage with respect to mass transfer from the solid phase to the liquid phase, since the dissolution rate can be increased by applying a proper agitation strategy. However, inherent to the design of stirred tank bioreactors, solid, hydrophobic particles cling to the agitation system, baffles and walls. This, together with lifting and separation of particles from the liquid phase by sparged air, required for the metabolism of the microbial cells, prevents the efficient biodegradation of solid PAHs (Gray et al., 1994). Application of a conventional roller bioreactor circumvents these problems to some extent (Brinkmann et al., 1998). The conventional roller reactor can be used in such a way as to minimize stripping

losses. This is generally accomplished by adding air only at certain intervals and leaving the reactor closed to the atmosphere the bulk of the time.

Biodegradation of naphthalene as a model PAH with *Pseudomonas putida* has been studied in previous work, both in the stirred tank and roller bioreactors (Purwaningsih et al. 2002). Although efficient solid to liquid mass transfer was achieved in the stirred tank bioreactor (volumetric mass transfer coefficient: 5 h^{-1}) the extensive stripping loss of naphthalene, due to splashing and aeration, made the use of a stirred tank bioreactor for biodegradation of naphthalene impractical. The stripping of naphthalene was overcome by using the conventional roller bioreactor but significant mass transfer limitations (volumetric mass transfer coefficient: 0.06 h^{-1}) prevented the efficient biodegradation of naphthalene. In order to fully realize the potential of a conventional roller bioreactor, means of increasing the mass transfer coefficients must be undertaken.

CHAPTER 3 THEORY

3.1 Mass Transfer

The mathematical model used in the calculation of the mass transfer rate is developed from the fundamental basis of film theory. The concentration gradient across the film is taken to be rapidly established in relation to the change in concentration within the bulk solution, so the flux is considered a constant at any given time (Mulder et al., 1998). At the solid particle's interface with the liquid, it is assumed that the solid and liquid phases are in equilibrium so that the concentration at the interface is equal to the saturation concentration. With this assumption in place the flux of the substance from the solid particle interface, *N* (mg dm^{-2} h^{-1}) into the bulk aqueous phase is described with a mass balance over a given thickness of the film:

$$N = \left(\frac{D}{\delta}\right)(C_L{}^* - C_L) \qquad (3.1)$$

In the above equation *D* is known as the diffusion coefficient and has units of m^2h^{-1}. $C_L{}^*$ is the saturation concentration of PAH adjacent to the solid and C_L is the bulk liquid concentration (mg L^{-1}). The symbol δ represents the thickness of the film. By convention, the ratio of the diffusion coefficient to the film thickness is commonly expressed as:

$$\frac{D}{\delta} = k_L \tag{3.2}$$

The term k_L in this equation is referred to as the film mass transfer coefficient (m h^{-1}). The change in concentration in the aqueous phase is caused by the flux, *N*. In equation form it follows that:

$$V \frac{dC_L}{dt} = NA \tag{3.3}$$

In the above equation, *V* refers to the aqueous phase volume (m^3), *A* is the total interfacial area between solid and liquid (m^2). If Equations 3.1 to 3.3 are combined we obtain:

$$\frac{dC_L}{dt} = \frac{A}{V} k_L (C_L{}^* - C_L) \tag{3.4}$$

Because it is almost always an extremely difficult proposition to accurately determine the total surface area of particles available for mass transfer, a combined form of mass transfer coefficient is used, often referred to as the volumetric mass transfer coefficient.

$$\frac{A}{V} k_L = k_L a \tag{3.5}$$

where $k_L a$ is the local overall mass transfer coefficient, liquid side (h^{-1}). This $k_L a$ can be readily found by integrating equation (3.4) with respect to time. Assumptions made include constant surface area of the particles and appropriate boundary condition such that the concentration of the dissolved compound (C_L) at time 0 is taken to be 0.

$$\ln\left(\frac{C_L^* - C_L}{C_L^*}\right) = -k_L a t \tag{3.6}$$

The volumetric mass transfer coefficient can be quickly obtained as the slope of the line obtained by plotting the function on the left hand side of the equation versus time. A simple model for the dissolution of polycyclic aromatic hydrocarbons to the liquid phase at any given time can then readily be obtained by rearranging Equation (3.6) as follows:

$$C_L = C_L^* \left(1 - \exp\left(-k_L a t\right)\right) \tag{3.7}$$

Mass transfer from the solid to the liquid phase is an extremely important step when attempting to biodegrade solid substances in a liquid slurry. Bacteria are unable to metabolize solid particles. The compound of interest must first enter the aqueous phase before being degraded.

3.2 Bioremediation

Bioremediation is a waste treatment approach utilizing biological processes. This includes the use of enzymes, bacteria, fungi, or plants to degrade, transform, sequester, mobilize or contain organics, inorganics or metallic pollutants. (McMillen et al., 2001). In order for bacterial remediation to occur, bacteria must be present in the medium. If the system is open and the compound to be remediated is volatile, a portion of the substrates will be lost to the surrounding air. This volatilized portion must be accounted for or erroneous estimates of the specific growth rate and microbial yield coefficient will be obtained. The effect of volatilization will be more pronounced for low solubility compounds because the percent of substrate lost will be higher.

In this discussion, stripping losses and volatilization will be neglected because air stripping in the roller bioreactor used was insignificant (Purwaningsih et al., 2004). Neglecting stripping losses, the rate of biomass formation and substrate uptake are connected according to equation (2.9), which can be rewritten as:

$$\frac{dX}{dt} = -Y_{X/S}\left(\frac{dC_T}{dt}\right) \tag{3.8}$$

In the above equation C_T refers to the total concentration of PAHs in the solution for both solid and aqueous phases (mg L^{-1}). Because the substrate is present in the aqueous phase as well as in the solid phase, the change in total substrate concentration is then:

$$\frac{dC_T}{dt} = \frac{dC_L}{dt} + \frac{dC_S}{dt} \tag{3.9}$$

The term C_S refers to the total solid concentration present in the reactor while C_L refers to the dissolved concentration. Substituting Equation (3.9) into (3.8), we obtain the following:

$$\frac{dX}{dt} = -Y_{X/S}\left(\frac{dC_L}{dt} + \frac{dC_S}{dt}\right) \tag{3.10}$$

For a biodegradation system employing bacteria, mass transfer is not rate limiting if the cell density is low while the available substrate concentration C_L is high (Volkering et al., 1992). Under these conditions exponential growth can occur. However, for high cell densities growing on a relatively insoluble substance it may be assumed that C_L is negligible compared to C_S. The time derivative $\frac{dC_L}{dt} \approx 0$, and equation (3.10) becomes:

$$\frac{dX}{dt} = -Y_{X/S}\left(\frac{dC_S}{dt}\right) \tag{3.11}$$

Under these conditions, mass transfer is the rate limiting step in the biodegradation process. This gives the equation:

$$\left(\frac{dC_S}{dt}\right)_{\max} = -k_L a C_L^{*} \tag{3.12}$$

When substrate is available in the system in a solid form, the rate of degradation by the bacteria present is unable to exceed the mass transfer rate. Therefore, biomass growth rate is limited by mass transfer. This can be expressed in a formula in the following manner:

$$\frac{dX}{dt} = Y_{X/S}(k_L a)C_L^* \qquad (3.13)$$

To better illustrate the theory presented in Equations 3.8 - 3.13 two graphs are presented. Figures 3.1 and 3.2 do an excellent job of showing the difference between a conventional biodegradation batch case where mass transfer is not rate limiting and the case where mass transfer is rate limiting.

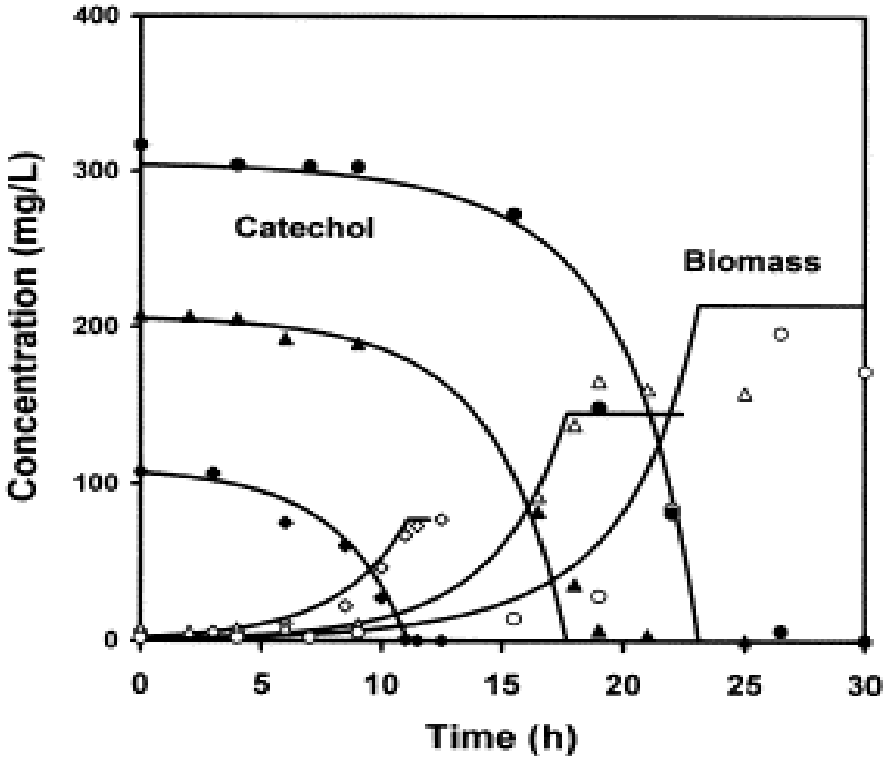

Figure 3.1: Standard biodegradation curve (Purwaningsih et al., 2002)

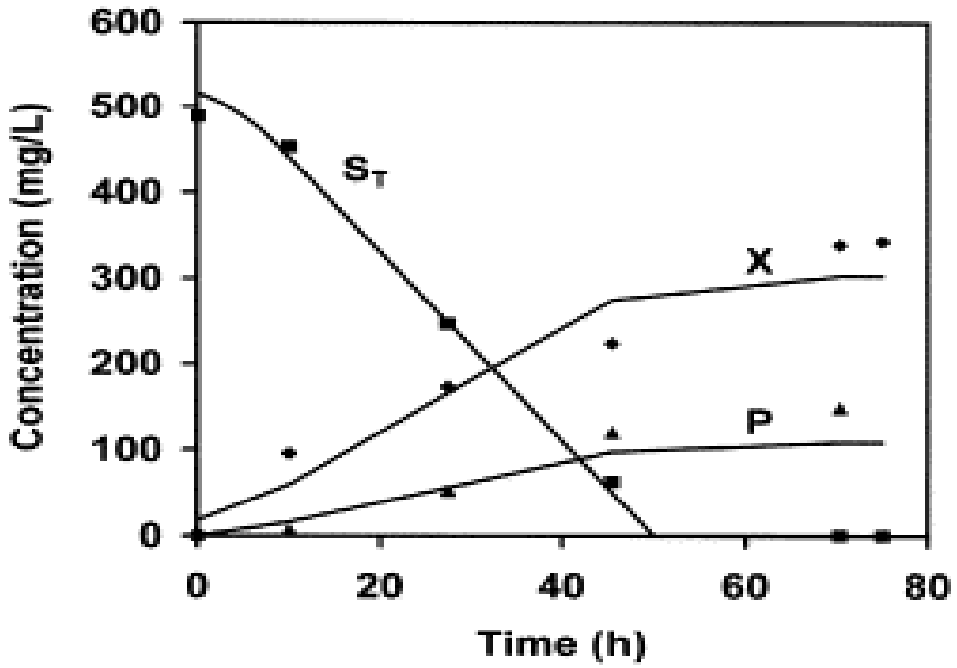

Figure 3.2: Mass transfer limiting biodegradation (Purwaningsih et al., 2002)

There is a marked difference in the biodegradation curves. In the conventional biodegradation curve, the substrate begins to slowly be consumed and then the rate of degradation becomes more and more rapid. The biomass curve follows the same trend, slowly building up to a period of exponential growth. In the mass transfer limited case, note that the substrate curve is linear as is the biomass growth curve. The substrate is being broken down as quickly as it enters the solution. A constant rate of degradation and/or biomass growth indicates a mass transfer controlled system.

CHAPTER 4 MATERIALS AND METHODS

4.1 Microorganisms, Medium and Chemicals

The polycyclic aromatic hydrocarbons used in the experiments carried out in the course of this work were naphthalene, 2-methylnaphthalene, and 1-5 dimethylnaphthalene. Naphthalene is a powdery white substance, while the methylnaphthalenes are more of a flaky yellow substance. These chemicals were all obtained at purities higher than 99% from Aldrich Chemical (Milwaukee, WI, USA). This is the same supplier used in earlier work with PAHs. All three of these compounds have specific gravities very close to 1 and are very hydrophobic. This means that they float on water and tend to clump together. This limits the surface area available for solid-liquid mass transfer.

The spherical glass beads (1, 3 and 5 mm) used as mass transfer aids were obtained from Potters Canada, Moose Jaw, Canada. The cylindrical glass Raschig rings (ID=3 mm, OD=6 mm, L=5mm) used were obtained from the lab reserves. The spherical glass marbles (15 mm) used as mass transfer aids were obtained from a local toy store. For a picture of the relative sizes of mass transfer aids, please refer to Figure 4.1.

The microorganism used in this study was *Pseudomonas putida* (ATCC 17484), obtained from the American Type Culture Collection, Virginia, USA. The Pseudomonads are known for their exceptional ability to degrade aromatic hydrocarbons (Bouchez et al., 1995). This aerobic bacterium is chemoheterotrophic with an optimum temperature growth range between 25 and 30 ^{o}C in a neutral pH environment. *P. putida* is a gram negative rod shaped

bacteria which is motile by means of flagellae. The bacterium was rehydrated from freeze-dried condition initially and the cells were stored on nutrient broth agar plates at 4 ^{o}C.

Figure 4.1 Mass transfer aids –from left to right: 3mm glass beads, Raschig rings, 5mm glass beads, 15mm marbles.

The microorganism used in this study was *Pseudomonas putida* (ATCC 17484), obtained from the American Type Culture Collection, Virginia, USA. The Pseudomonads are known for their exceptional ability to degrade aromatic hydrocarbons (Bouchez et al., 1995). This aerobic bacterium is chemoheterotrophic with an optimum temperature growth range between 25 and 30 ^{o}C in a neutral pH environment. *P. putida* is a gram negative rod shaped

bacteria which is motile by means of flagellae. The bacterium was rehydrated from freeze-dried condition initially and the cells were stored on nutrient broth agar plates at 4 ^{o}C.

The mineral nutrient medium used to support the growth of *P. putida* ATCC 17484 was McKinney's modified medium, as used by Hill and Robinson (1975). The composition of the minerals for one liter of growth medium is demonstrated in Table 4.1. One ml of trace element solution (Table 4.2) was added per liter of medium. The final pH of the medium was 6.8. The medium was prepared by mixing the inorganic chemicals into one liter of reverse osmosis water. This mixture was then sterilized at 121 ^{o}C for 30 minutes to kill any contaminating organisms.

Table 4.1: Growth media minerals in 1 liter of reverse osmosis water

SUBSTANCE	WEIGHT (mg)
KH_2PO_4	420
K_2HPO_4	375
$(NH_4)_2SO_4$	237
NaCl	30
$CaCl_2$	30
$MgSO_4$	30
$Fe(NH_4)_2SO_4$	10

Table 4.2: Trace element composition in 1 liter of reverse osmosis water

SUBSTANCE	WEIGHT (mg)
H_3BO_3	300
$CoCl_3$	200
$ZnSO_4.7H_20$	100
$MnCl_2$	30
Na_2MoO_4	30
$NiCl_2$	20
$CuCl_2$	10

Liquid cultures were prepared by transfer of bacterial colonies from agar plates to 125 ml of a sterile McKinney's modified medium containing 250 mg/l of particulate naphthalene as growth substrate in 250 ml Erlenmeyer flasks. These flasks were then placed on a rotary shaker at 200 rpm at room temperature. Once the bacteria reached the exponential growth phase, these flasks were used to inoculate the experimental runs and were also used to propagate bacteria on fresh plates. The stock liquid cultures were maintained by subculturing on a bi-weekly basis.

Agar plates were prepared by the addition of 3 grams of bacto-agar to 100 ml distilled water. Nutrient broth was added (0.8 grams) and also 20 mg of naphthalene to guard against possible contamination. These ingredients were stirred while heating on a hot plate until just about the boiling point and were then

sterilized for 30 minutes at 121 ^{o}C. After sterilization, the solution was poured into Petri dishes inside the biofilter cabinet hood. In order to propagate bacteria on fresh agar, several loops of broth solution from the shake flask were aseptically removed and streaked on agar plates. These plates were renewed every two weeks to ensure a fresh source of microbes.

4.2 Experimental Apparatus

Roller bioreactors were 2.5 liter, narrow mouthed glass jars (inside diameter of 12.5 cm, length of 21 cm), rotated on a Bellco Biotechnology roller apparatus (model 7622-S0003, New Jersey, USA). This Bellco apparatus is a bi-level, multiple speed unit which has 6 roller bars and a heavy duty DC motor. The pulleys are connected in such a way that once the motor begins, all rollers rotate simultaneously.

The bioreactors were operated with one liter working volume at room temperature of 22 ± 1 ^{o}C and at a rotation speed of 50 rpm. Teflon caps, placed over the roller jar openings, allowed sampling and intermittent injection of air into the bioreactors. The caps were equipped with filtered air vents. A sketch of the roller apparatus is provided in Figure 4.2 and a picture of the conventional roller reactor is shown in Figure 4.3.

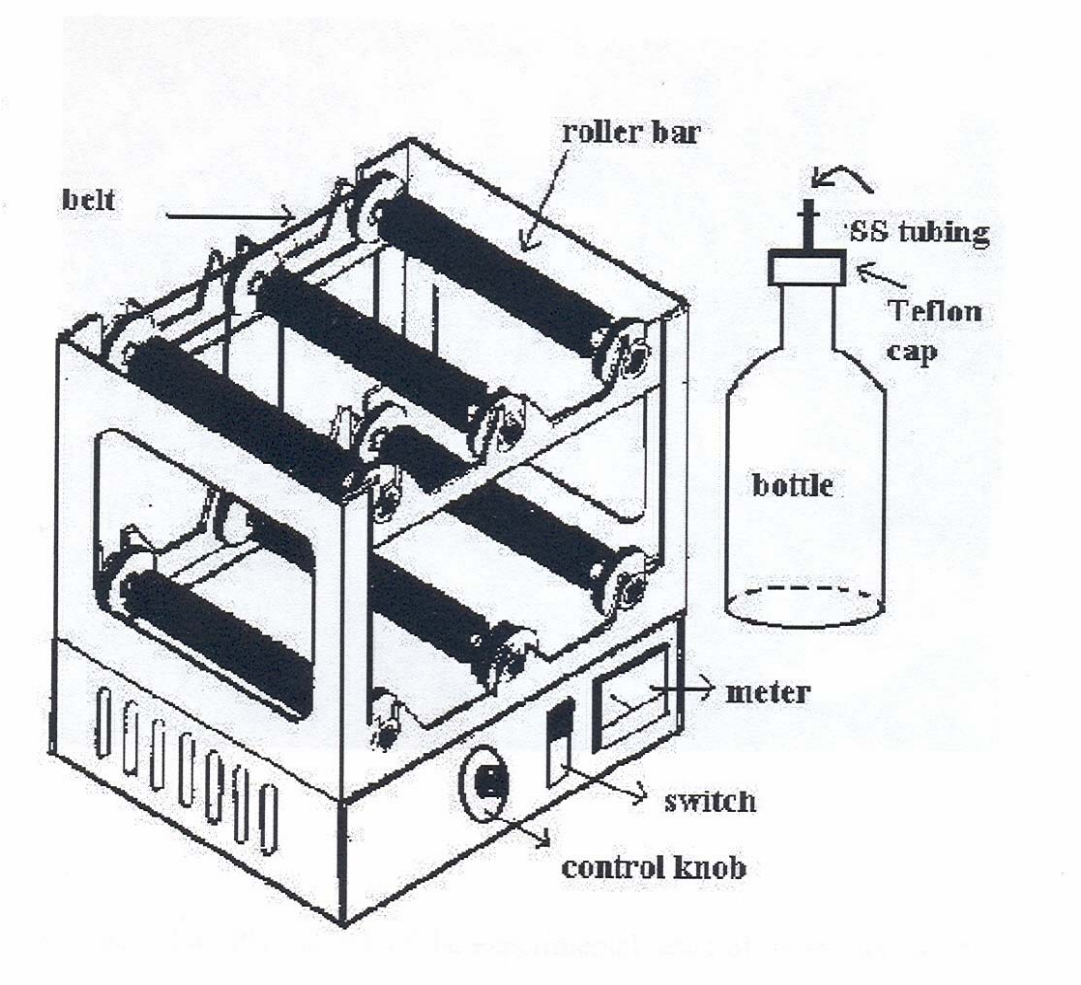

Figure 4.2 Bellco roller apparatus

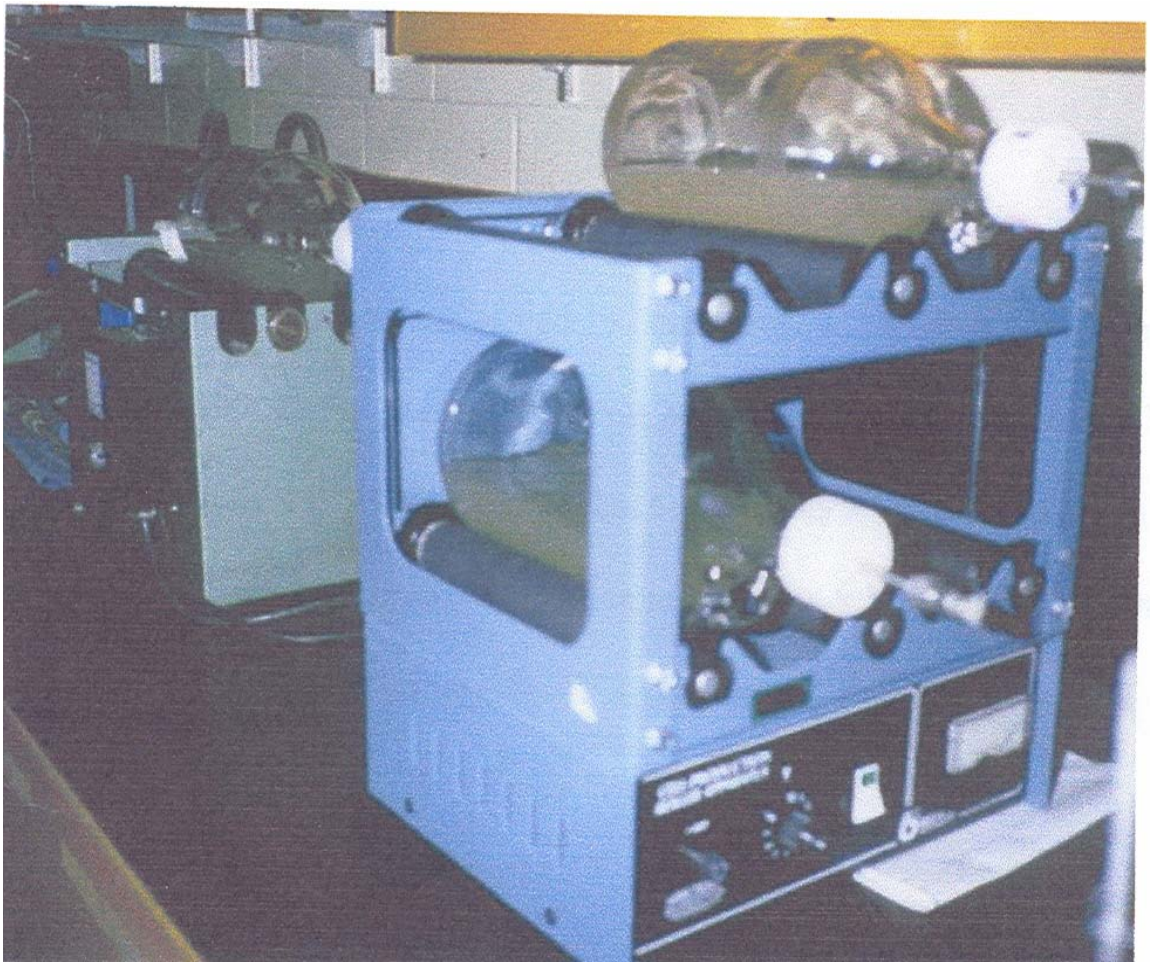

Figure 4.3 Picture of the experimental setup – conventional roller reactor

Two different sizes of reactor were used in scale up studies. The bioreactor of intermediate size had a volume of 20 L (inside diameter of 25cm, length of 42 cm).and was operated with a working volume of 8 L. The largest reactor used had a total volume of 58.5 L (inside diameter 39cm, length of 55cm), and was operated with a working volume of 23L. For scale up biodegradation experiments, the roller apparatus was driven by a 3 hp Marathon Electric MicroMax continuous duty motor. The scaled up reactors were rotated at

50 rpms regardless of diameter. For a visual comparison of reactor size, see Figure 4.4. The rotation speed was controlled by a Mitsubishi inverter. A picture of the scale up apparatus is shown in Figure 4.5.

Figure 4.4 Reactor comparison left to right – bead mill bioreactor, 23 L reactor, 58 L reactor.

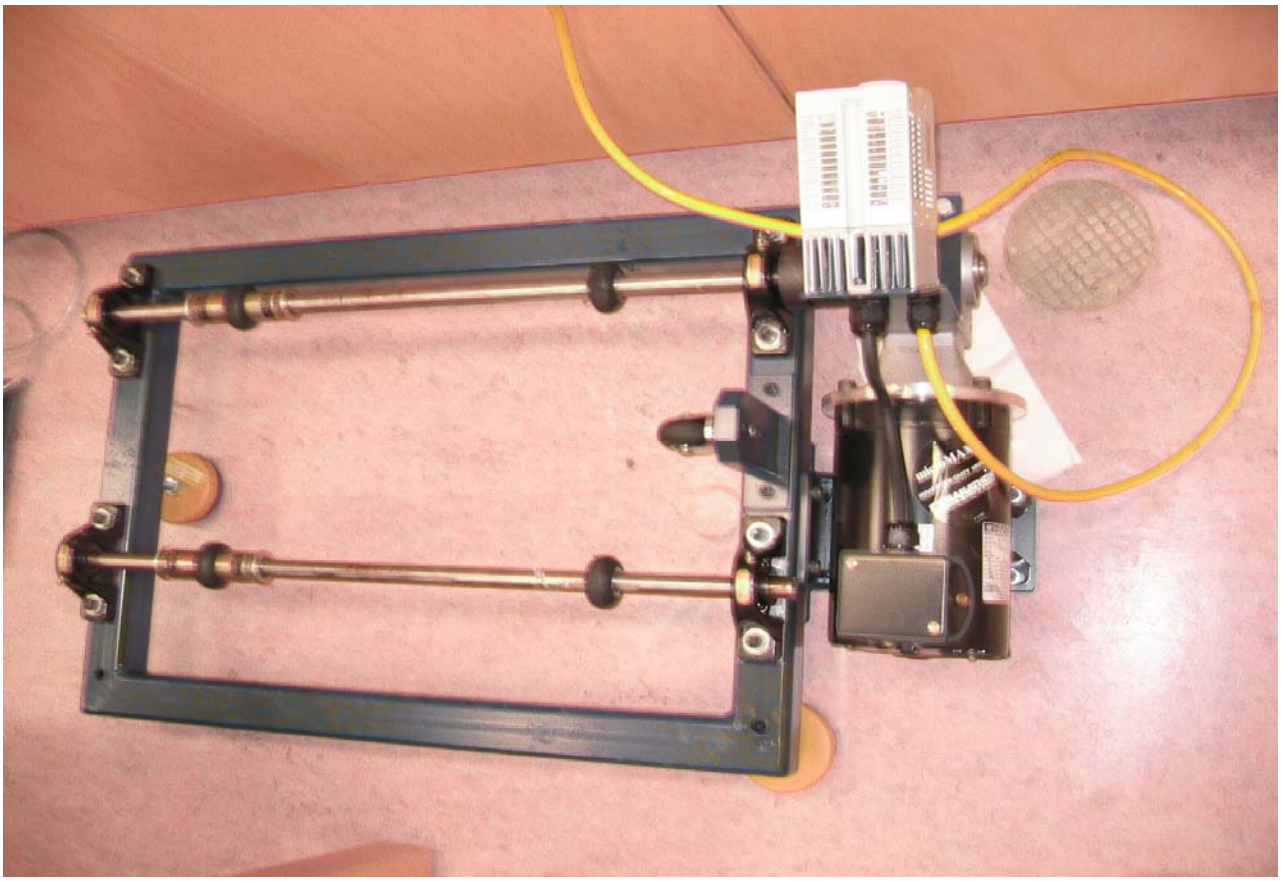

Figure 4.5 Scale up roller apparatus used in the scale-up studies

4.3 Procedures

4.3.1 Mass Transfer Experiments

Because it was determined in previous work that the rate-limiting step for biodegradation in a roller reactor was mass transfer (Purwaningsih et al., 2004), it was necessary to quantify the mass transfer rate and to attempt to improve upon it. To determine the dissolution rate of solid PAH particles, experiments were carried out by inserting particles into 1 L working volume (reverse osmosis water + inert particles) at room temperature. The experimental variables studied using the roller apparatus were PAH particle concentration, inert particle loading, inert particle size and type and PAH type. Prior to beginning any mass transfer

or biodegradation experiments, PAH particles were ground and sieved to a diameter of less than 100 microns. The mean diameter was found to be 80 microns.

Initial experiments were carried out using naphthalene as a model PAH. The concentration of naphthalene was varied from 500 mg/L to 10000 mg/L based on water volume. To assess the effect of particle loading on the extent of mass transfer various quantities of 3 mm glass beads (10, 25, 50, 75%; volume of glass beads/total working volume) were added to the roller bioreactors containing McKinney's modified medium and 1000 mg/L of suspended naphthalene particles. The effect of bead size on the extent of mass transfer was investigated using glass beads with diameters of 1, 3 and 5 mm. To see the effects of a different inert particle, in one set of experiments glass Raschig rings (ID=3 mm, OD=6 mm, L=5mm) were used instead of glass beads. In all cases control experiments were carried out under identical operating conditions and in the absence of glass beads or Raschig rings.

The concentration of the PAH in solution was measured during the course of mass transfer experiments, and samples were obtained from the reactor at desired times. In order to determine dissolved concentrations, samples were filtered through a 0.2 μm mixed cellulose ester membrane, followed by quantification using a Hewlett-Packard 1100 series HPLC.

4.3.2 Biodegradation Experiments

The glass reactors were first carefully loaded with the desired amount of RO water, nutrient media (see Tables 4.1 and 4.2), and inert particles. This mixture was then sterilized at 121 ^{o}C for 60 minutes in order to remove any contaminating organisms. The inoculum for the experiments was prepared in shake flask as described in Section 4.1. When the inoculum reached the exponential growth stage, 30 ml of inoculum was added to the reactor along with 250 mg of PAH compounds. This gave a liquid concentration of 500 mg/L since half of the working volume was occupied by beads. The total working volume of the reactor was in all cases precisely 1 L to avoid introducing unnecessary differences in experimental conditions. The concentration of total naphthalene was determined periodically. At each sampling time, 10 ml representative samples were obtained by vigorously shaking the reactor for 1 minute and then pouring out the desired sample. A 5 ml portion of this sample was immediately diluted in 10 ml of ethanol, and the resulting mixture was analyzed by HPLC. The dilution was necessary because the total naphthalene concentration was far above the dissolved concentration in the slurry. The remaining 5 ml was used to determine the biomass concentration. Samples were always taken and analyzed in duplicate.

For scale up biodegradation experiments, every effort was made to create conditions similar to those used with the small bioreactor. The temperature and the rotation speed were the same. The working volume was also set at 40% of the total volume as it was for the smaller reactor (1L/2.5L). Precisely 50% of the

working volume was occupied by glass marbles. For the control condition, an overhead stirrer was used to mix the content of the bioreactor prior to sampling to ensure a representative slurry sample was obtained, as the reactors were too large to shake by hand. In the presence of the marbles, sampling took place with the reactor running, which ensured a sufficient mixing in the bioreactor during the sampling. The mass transfer aids used were 15 mm marbles. Air was also added continuously to the head space above the liquid.

4.3.3 Biomass Concentration Measurements

Biomass measurements were made by using a Milton Roy UV spectrophotometer (model 1001). The dry weight biomass concentration was related to the optical density by using a previously determined calibration curve. This curve was obtained by finding the biomass concentration using a dry weight method. A shake flask with 500 ml of bacterial culture grown on naphthalene was allowed to reach high biomass concentrations. Then 200 ml of this broth solution was placed in centrifuge tubes and centrifuged at 10000 rpm for 15 minutes in order to precipitate the organisms at the bottom of the tube. The resulting supernatant was then removed. Several drops of distilled water were then added followed by mixing using the vortex mixer. The procedure of centrifuging, decanting and rinsing were repeated. The resulting small amount of concentrated biomass solution was placed in pre-weighed aluminium dishes which were subsequently placed into a vacuum oven at 65 ^{o}C and -22 in Hg for 24 hours. The dishes were then placed in the dessicator for 1 hour in order to cool down the dishes to room temperature. The resulting change in weight from

the dried dish with biomass was compared to the dish alone and then used to calculate the original biomass concentration (mg per liter of broth). Samples of the same broth were diluted numerous times and analyzed for optical density. The resulting measurements provided a range of known biomass concentrations vs. optical densities and were used to construct the dry-weight-optical density calibration curve for *Pseudomonas putida*. If samples ever exceeded this range of calibration, they were simply diluted until the reading fell within the desired range.

4.3.4 Substrate Concentration Measurements

A High Performance Liquid Chromatograph (HPLC, Hewlett Packard model 1100) was employed to determine naphthalene concentration. The HPLC was equipped with an Agilent 1100 series auto sampler. A 20 µl volume of sample was injected on a 15 cm C18 NovaPak column (Waters) at a temperature of 25 ^{o} C. The mobile phase, a 50/50% (v/v) mixture of MiliQ-water (Millipore, USA) and acetonitrile, was pumped through the column at a flow rate of 2.1 ml/min and an average column pressure of 147 bar. A UV detector at 254 nm was used for the detection and analysis of the samples. In order to protect the HPLC column from chemical and particulate contamination in the mobile phase stream, a Waters Guard Pak^{TM} insert was used by connecting the Guard-Pak inlet to the injector and the outlet unit to the cartridge. Using known particulate slurry concentrations up to 1000 mg/L, this technique for measuring naphthalene concentration was found to be accurate and reproducible to within ± 2%.

4.3.5 Toxicity Measurements

Toxicity tests were performed on the untreated slurry and the treated effluent of the largest scale-up experiment performed (23L working volume). The untreated slurry was easily obtained by mixing 500mg/L naphthalene with water in the absence of bacteria or inorganic nutrients for several days. The treated effluent was taken directly from the reactor after 12 hours from inoculation. The control consisted of reverse osmosis water obtained in the laboratory.

The different steps of the toxicity tests were as follows (Toussaint et al., 1995). First one gram of brine shrimp eggs purchased from Petland were added to one hundred ml of RO water containing 25 g/L NaCl. This flask was kept at room temperature and was aerated for approximately 36 hours. After 36 hours, 0.5 ml of the brine shrimp solution were added to each of six watch glasses. Two ml of reverse osmosis water was added to the first two watch glasses and used as control. Two ml of a saturated naphthalene solution were added to the next two watch glasses and finally two ml of the bioreactor effluent (collected at the end of bioremediation run) was added to another two watch glasses. In all cases, the solutions added to the shrimp solution had NaCl added to bring the concentration to 25 g/L to ensure that shrimp were not dying due to lack of salt concentration. All motile shrimp were counted using a 7X magnification Optivisor headset pictured in Figure 4.6. Shrimp moving were said to be alive, while those not moving were said to be dead and were not counted. Shrimp numbers were observed at four times; 0, 0.5, 1 and 2 hours.

Figure 4.6 Optivisor 7X magnification headset

CHAPTER 5 RESULTS AND DISCUSSION

5.1 Mass Transfer Experiments

The bioavailability of PAHs has a profound effect on their biodegradation rate. Quite simply, if PAHs are not dissolved, they cannot be degraded by bacteria. In previous work it was demonstrated that mass transfer was the rate limiting step in biodegradation of PAHs in a roller bioreactor (Purwaningsih et al., 2004). Thus the first step in the present work was to find a simple, economical means of increasing the mass transfer rate in the roller reactor thereby increasing the biodegradation rate. In all cases the reactors were rotated at 50 rpm at room temperature, 22 ± 1 ^{o}C. The rotation rate of 50 rpm was found to be the optimum rotation rate in an earlier study (Purwaningsih et al., 2002). To determine the dissolution rate of solid PAH particles, experiments were carried out by including particles into 1 L working volume (distilled water + inert particles). The experimental variables studied using the roller apparatus were PAH particle concentration, inert particle loading, inert particle size and type, and PAH type. Other variables such as temperature, pH and the size of PAH particles were held constant in order to isolate the desired mass transfer effects.

5.1.1. Effects of inert particle loading

Initial experiments were carried out using 3 mm glass beads. Glass beads were readily available and inexpensive. Visual observations indicated a dramatic increase in turbulence within the reactor upon addition. Mass transfer experiments were carried out initially at a naphthalene concentration of 1000 mg/L, based on the volume of the liquid. The results are shown in Figure 5.1.

The dashed line indicates saturation concentration of the particular compound under experimentation in all mass transfer graphs.

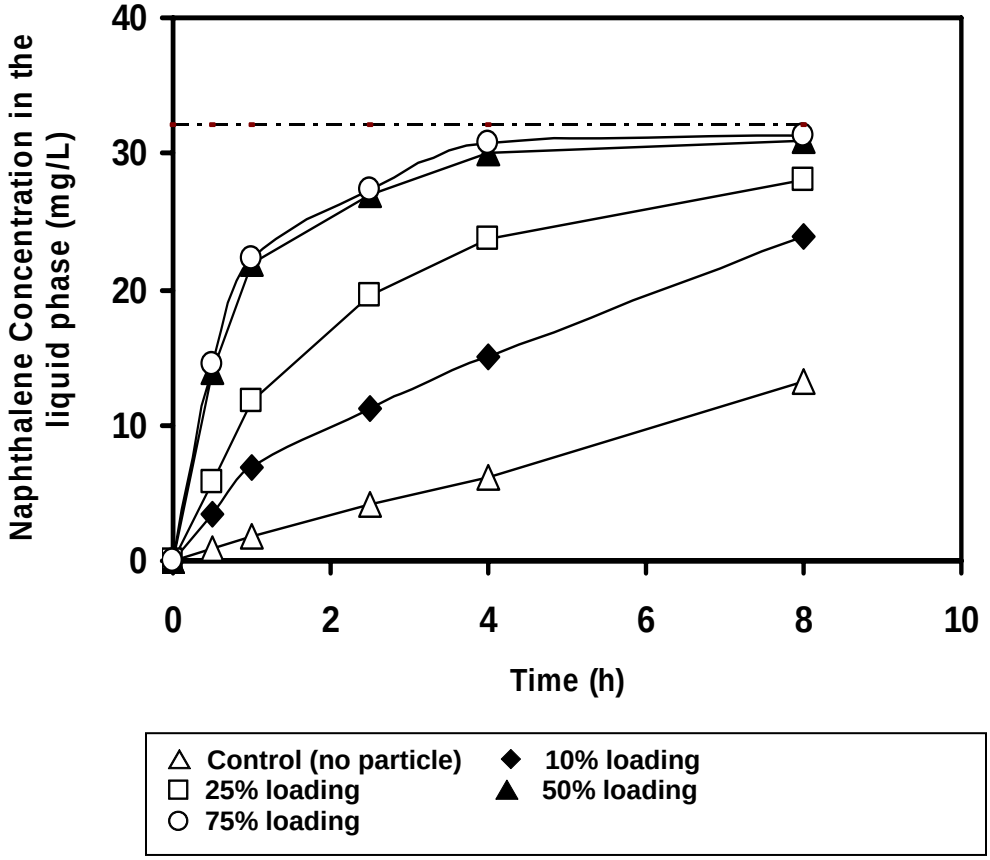

Figure 5.1 Dissolution of 1000 mg/L particulate naphthalene at different loadings of 3mm glass beads

As expected, the dissolution rate increased as the bead loading increased. However, this was true up to a certain point. Glass bead loadings of 75% resulted in mass transfer rates nearly identical to those observed at 50%. Because the liquid volume available for biodegradation would be small at 75% loading, 50% loading was used as the optimum value. Up to 50% loading, the addition of glass beads noticeably increases the turbulence in the reactor. The

beads were carried up the walls of the reactor and fell back down into the liquid as well as moving back and forth in an oscillatory manner. Due to mixing, the beads increase the particle surface area contacting the liquid through grinding the PAHs into smaller particles, increasing the surface area available for mass transfer between the solid and liquid. Although not quantified in this work the created turbulence should have a positive effect on the mass transfer between the gas and liquid as well.

In order to reach the liquid phase, PAH molecules are forced to travel through the solid-liquid resistance film discussed in Chapter Three. The increased mixing and turbulence in the reactor due to inert particles had the desired effect of decreasing the film thickness and increasing the mass transfer rate. Mulder et al., (1998) demonstrated a similar result by using impeller speed in a well-mixed reactor. They found that by increasing impeller speed from 30 to 75 rpm, the film thickness was reduced by a factor of 3. As can be seen from Equation (3.2), the mass transfer coefficient of the film is inversely proportional to the thickness of the film. Purwaningsih et al., (2002) showed that by increasing the rotational speed of a conventional roller bioreactor from 20 to 50 rpm, the mass transfer increased by a factor of 2. Increases in turbulence and mixing clearly lead to greater mass transfer rates from the solid and gas phases into the liquid phase. These increases in mass transfer can in many cases translate directly into increased rates of biodegradation which is a highly desirable outcome.

5.1.2 Effect of Solid PAH concentration

Once the effect of bead loading on the dissolution rate was determined it was decided to investigate the effect of initial PAH particle concentration in conjunction with bead loading. To this end, experiments were carried out at 500, 1000, 5000 and 10000 mg/L initial PAH particle concentrations. The graphs summarizing these results can be found in Figures 5.2, 5.1, 5.3 and 5.4 respectively.

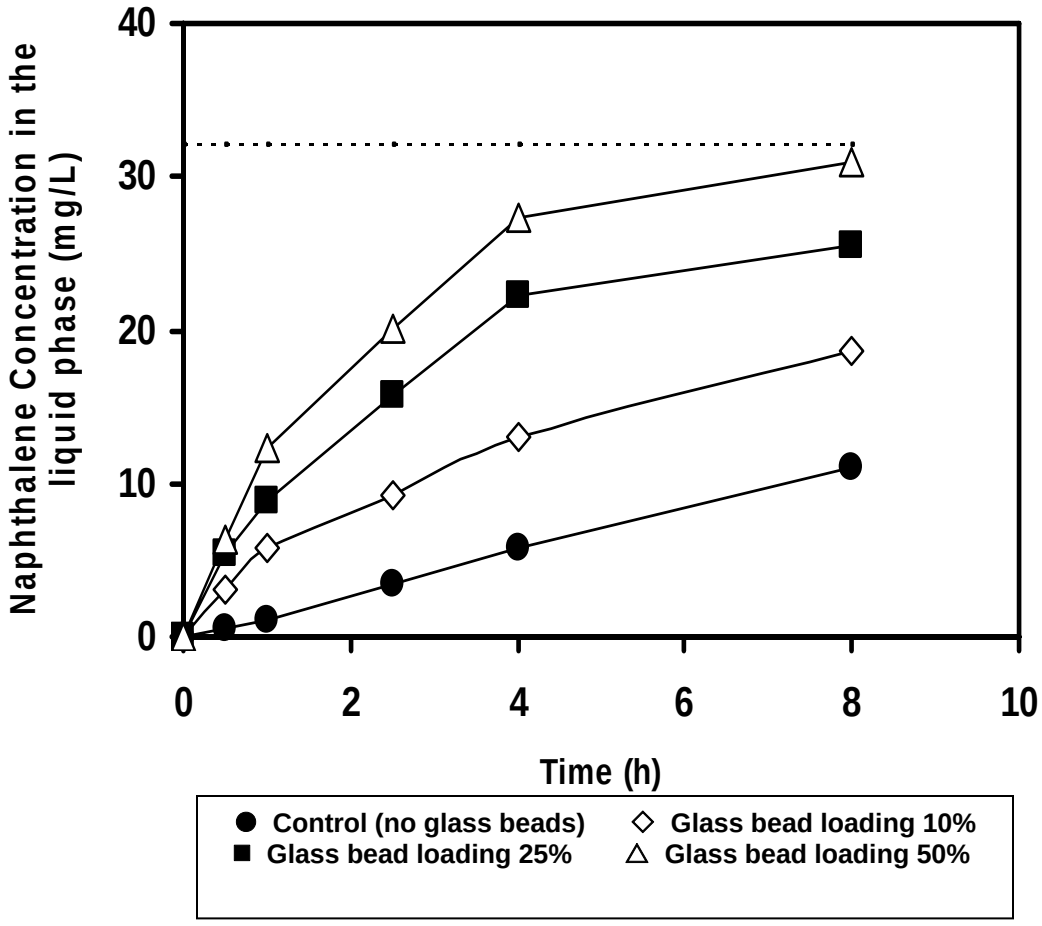

Figure 5.2 Dissolution of 500 mg/L particulate naphthalene at different loadings of glass beads

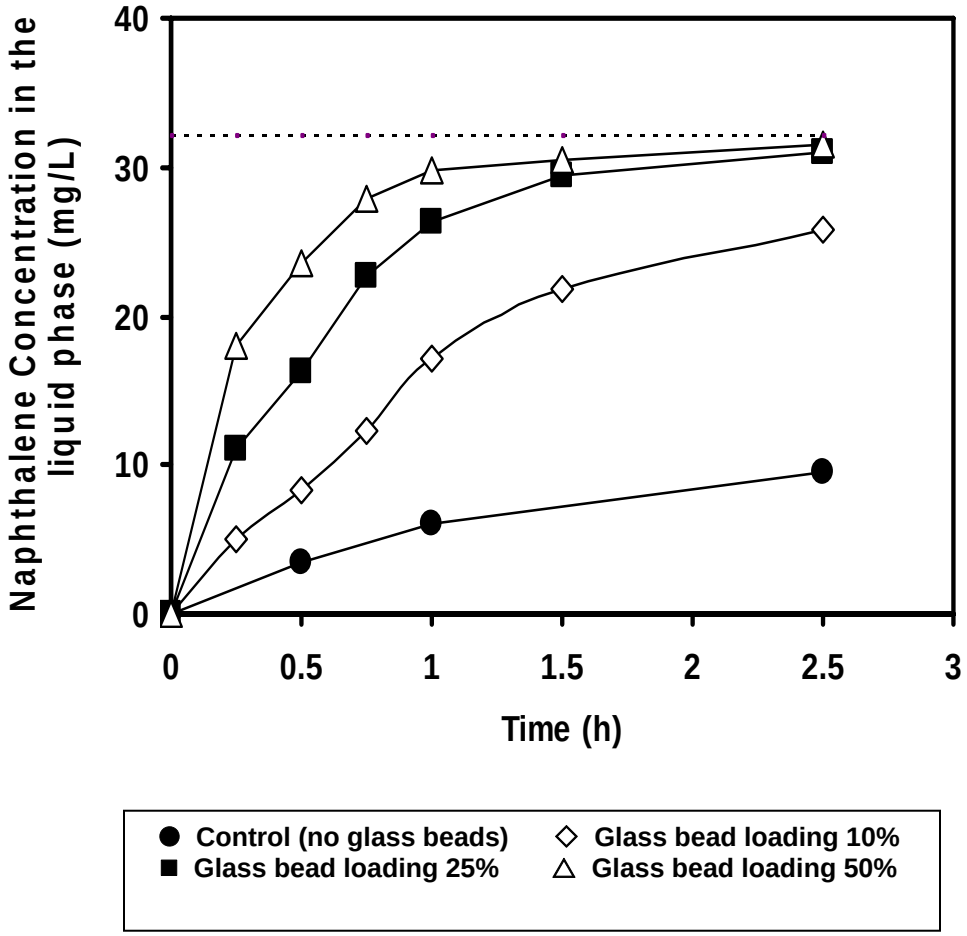

Figure 5.3 Dissolution of 5000 mg/L particulate naphthalene at different loadings of glass beads

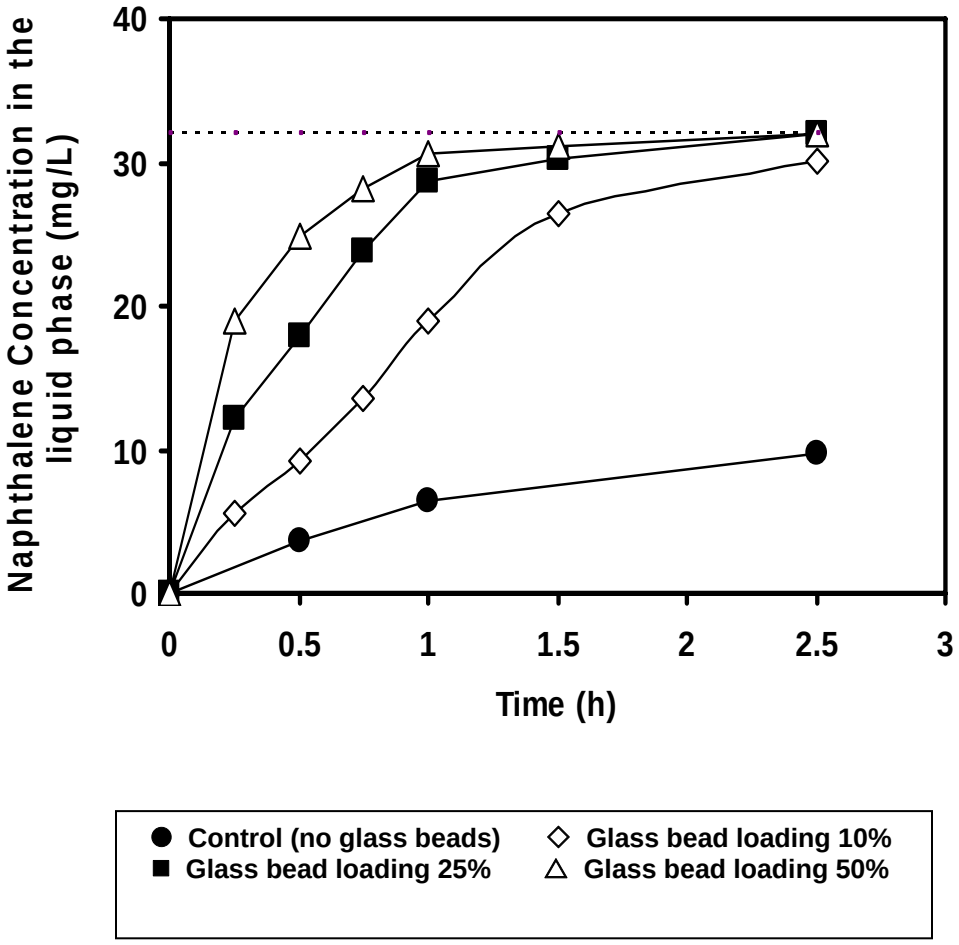

Figure 5.4 Dissolution of 10000 mg/L particulate naphthalene at different loadings of glass beads

As expected, as the amount of naphthalene in the system increased, the time required to reach saturation decreased. This is because of the increasing surface area available for mass transfer. Clearly, mass transfer rates increase with increased PAH particle loading as well as with increased bead loading.

In order to quantify the effects of glass bead loading on the extent of mass transfer, the experimental data were fit into Equation (3.6) and the overall volumetric mass transfer coefficient (k_La) was calculated. The slope of the line created when plotting the logarithmic function vs. time was taken to be $k_La(h^{-1})$. Figure 5.5 illustrates the calculation of k_La for 5mm beads and 500mg/L of naphthalene.

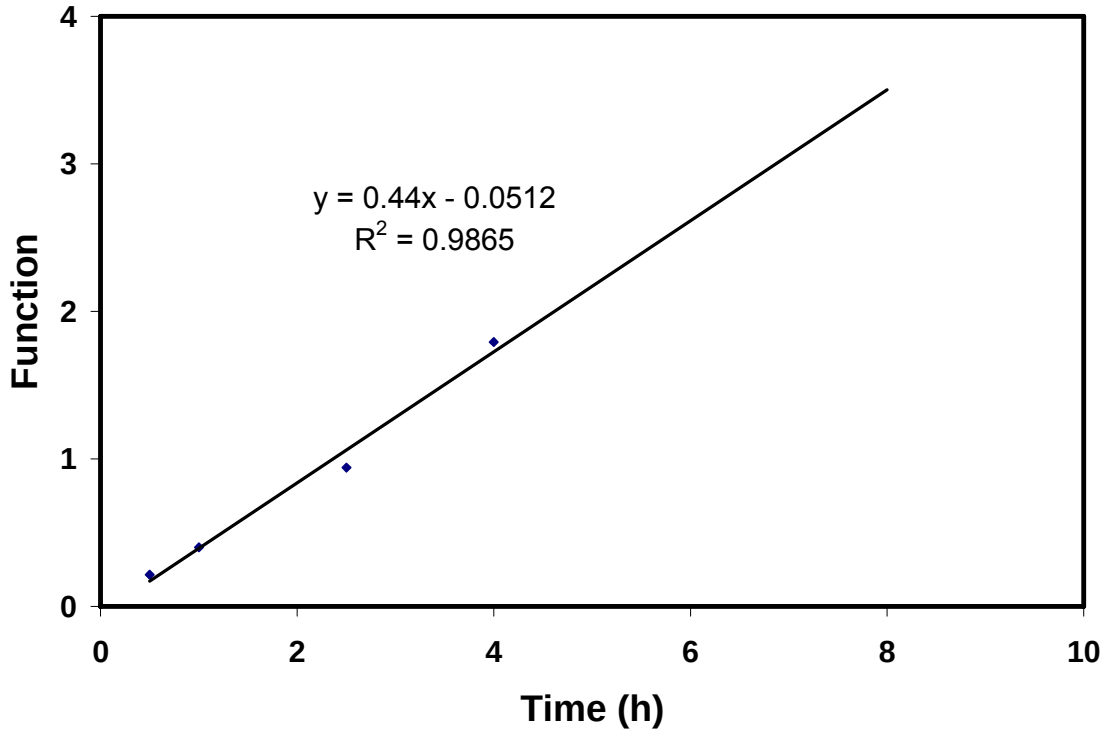

Figure 5.5 Calculation of k_La for 500mg/L naphthalene, 50% 5 mm beads.

The function on the left hand side of the graph is: $\ln\left(\frac{C_L^* - C_L}{C_L^*}\right)$

This function is the left hand side of Equation 3.6.

Using the experimental data, the values of k_La were determined under each condition. Figure 5.6 plots the volumetric mass transfer coefficient k_La as a function of initial naphthalene concentration. The results clearly demonstrate that the mass transfer rate increases as the particle concentration increases. At the optimum bead loading of 50%, the mass transfer rate rises from a low value of 0.44 h^{-1} at an initial concentration of 500 mg/L to a high level of 2.1 h^{-1} at initial concentration of 10000 mg/L. This result shows a similar trend that other researchers have observed (Mulder et al., 1998, Purwaningsih et al., 2004) and that is predicted by the theory. Mulder observed that by increasing the amount of solid naphthalene present in the aqueous system, the dissolution rate was increased. The higher concentration of particles present in the solution creates a greater surface area for interaction between the solid particles and the bulk liquid phase. The increase in area means that the term k_La is increasing, although k_L itself may be constant.

In this study a twenty times increase in the particle concentration resulted in a five times increase in the volumetric mass transfer coefficient observed. This is a dramatic increase in mass transfer when compared to the increase observed by Purwaningsih et al., (2002). They observed that a four times increase in particle concentration resulted in only a 20% increase in the volumetric mass transfer coefficient. In the current work, a four times increase in PAH particle concentration resulted in mass transfer increases of about 90%. This demonstrates the dramatic effects that the introduction of inert particles in the

system can have when compared to an identical system in the absence of glass beads.

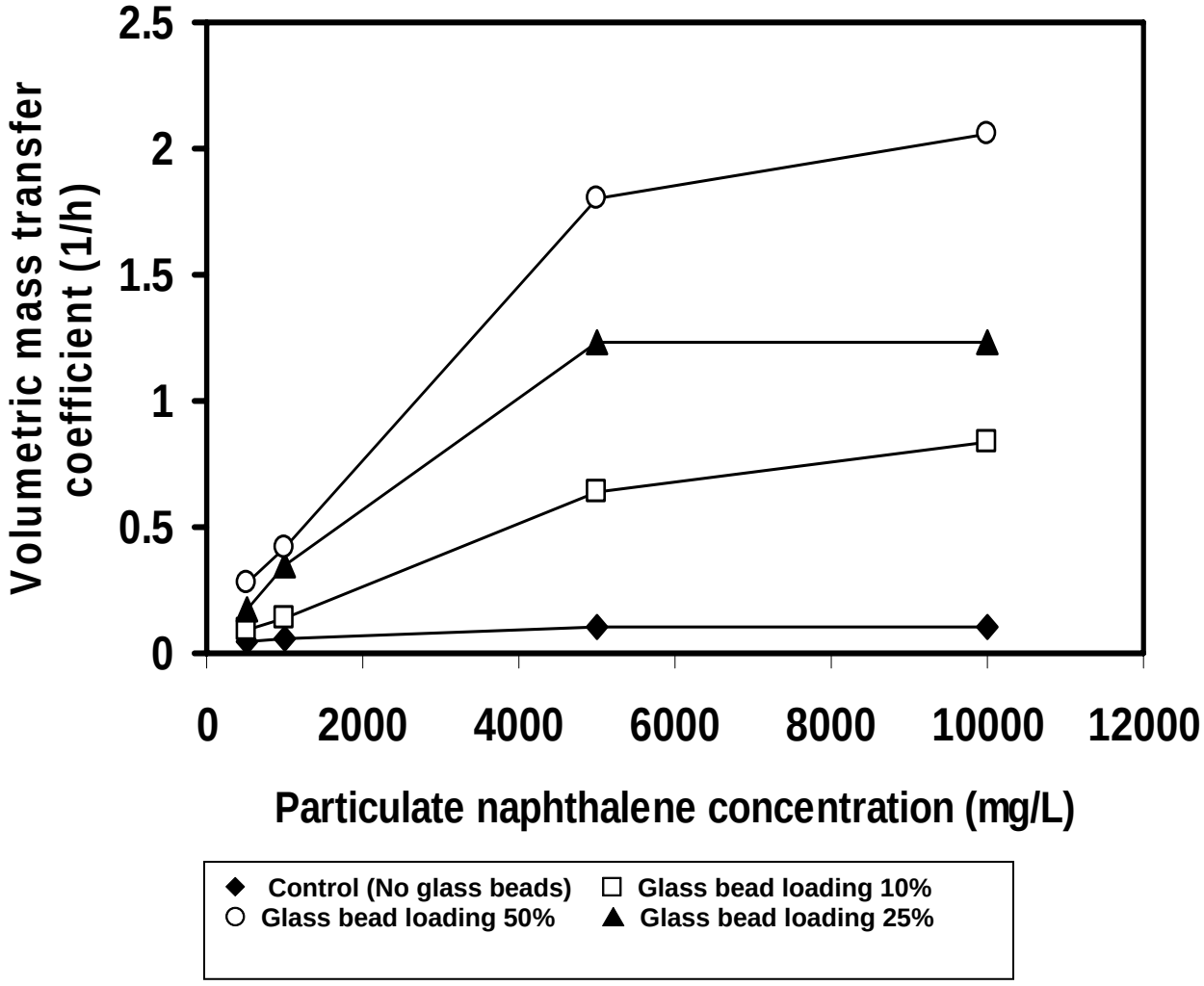

Figure 5.6 Dependency of volumetric mass transfer coefficient on concentration of particulate naphthalene and loading of 3 mm glass beads

5.1.3 Effects of size and type of inert particles (mass transfer enhancers)

The effects of the type and size of inert particles loading were investigated by using 1 mm, 3 mm, 5 mm spherical glass beads and 3 mm Raschig rings. The results of these experiments at 1000 mg/L naphthalene are shown in Figure 5.7. The volumetric mass transfer coefficient determined in the presence of Raschig rings, 1 mm, 3 mm and 5 mm glass beads were 0.31, 0.42, 0.58 and 0.70 h^{-1}, respectively. These values of $k_L a$ indicate that the use of glass beads is superior to Raschig rings as a mass transfer enhancer. The Raschig rings were visually observed to be less effective for creating turbulence. They floated on top of the liquid for the most part and were not carried up along the sides of the reactor to splash back down into the water. They also failed to induce the oscillatory motion that was evident when glass beads were utilized. Overall, they seemed to be too light for the application and tended to trap air bubbles in their cavity which prevented their submersion below the air-water interface.

The optimum conditions for mass transfer were found to be 50% loading of 5 mm glass beads. Clearly, the larger glass beads are more effective as a mass transfer aid than smaller diameter glass beads. The data suggests however that the effects of the increase in bead size lessen as the glass beads grow larger. There is a pronounced jump in $k_L a$ when increasing the bead size from 1 mm beads to 3 mm beads, while the difference between 3 mm beads and 5 mm beads is less significant. After one hour of experiment,

the 1 mm beads produced a concentration of 16.3 mg/L, while with 3 mm and 5 mm beads concentrations of 21.9 and 23.1 mg/L were achieved, respectively. As the size of the inert particles increased, the mass transfer gains obtained from their size seemingly became less significant.

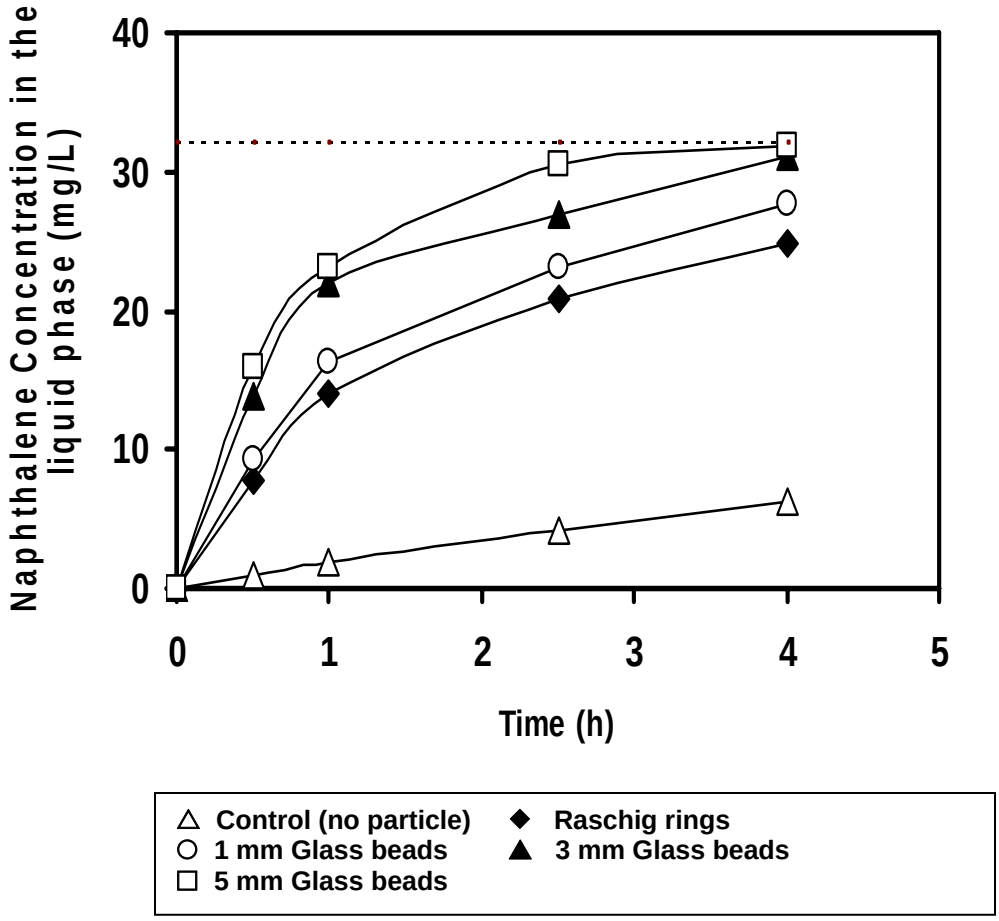

Figure 5.7 Dissolution of 1000 mg/L of particulate naphthalene in the presence of Raschig rings and glass beads of different sizes (particle loading: 50%).

5.2 Biodegradation of Naphthalene

Once the optimum conditions for naphthalene mass transfer were determined, the biodegradation of naphthalene was investigated under those conditions. The results of biodegradation of 500 mg/L of particulate naphthalene in a roller bioreactor with no beads, and in the presence of 5 mm glass beads at two different loadings of 25 and 50% are presented in Figure 5.8. Biodegradation of naphthalene in the roller bioreactor with no beads proceeded at a relatively constant rate of 10.6 $mgL^{-1}h^{-1}$ and was completed in 48 hours. The maximum degradation rate was taken to be the slope of the line of decreasing substrate once the bacteria reached exponential growth. The constant slope of the decline in naphthalene concentration indicates that mass transfer was rate-limiting. In the presence of glass beads the biodegradation rate was significantly faster than that observed in the control system, with the rate of biodegradation being dependent on the loading of the beads. With 25% loading, complete removal of 500 mg/L naphthalene was achieved in under 17 hours, while application of beads at a loading of 50% reduced the required time for complete removal of the naphthalene to just less than 9 hours. The corresponding biodegradation rate at 25 and 50% particle loadings were 62.8 and 118.4 $mgL^{-1}h^{-1}$, respectively. The biodegradation rates using the optimum mass transfer conditions were eleven times greater when compared with the control and the mass transfer rates at the initial loading of 500 mg/L increased by a factor of almost ten when compared to the control. Because this is a mass transfer controlled biodegradation, the gains

in mass transfer are very nearly directly applicable to the measured maximum degradation rate. The additional increases can be attributed to surfactants produced by the bacteria (Purwaningsih, 2002). All biodegradation graphs following omit the first three hours, or lag phase from the graphs so as to treat the data as a linear degradation.

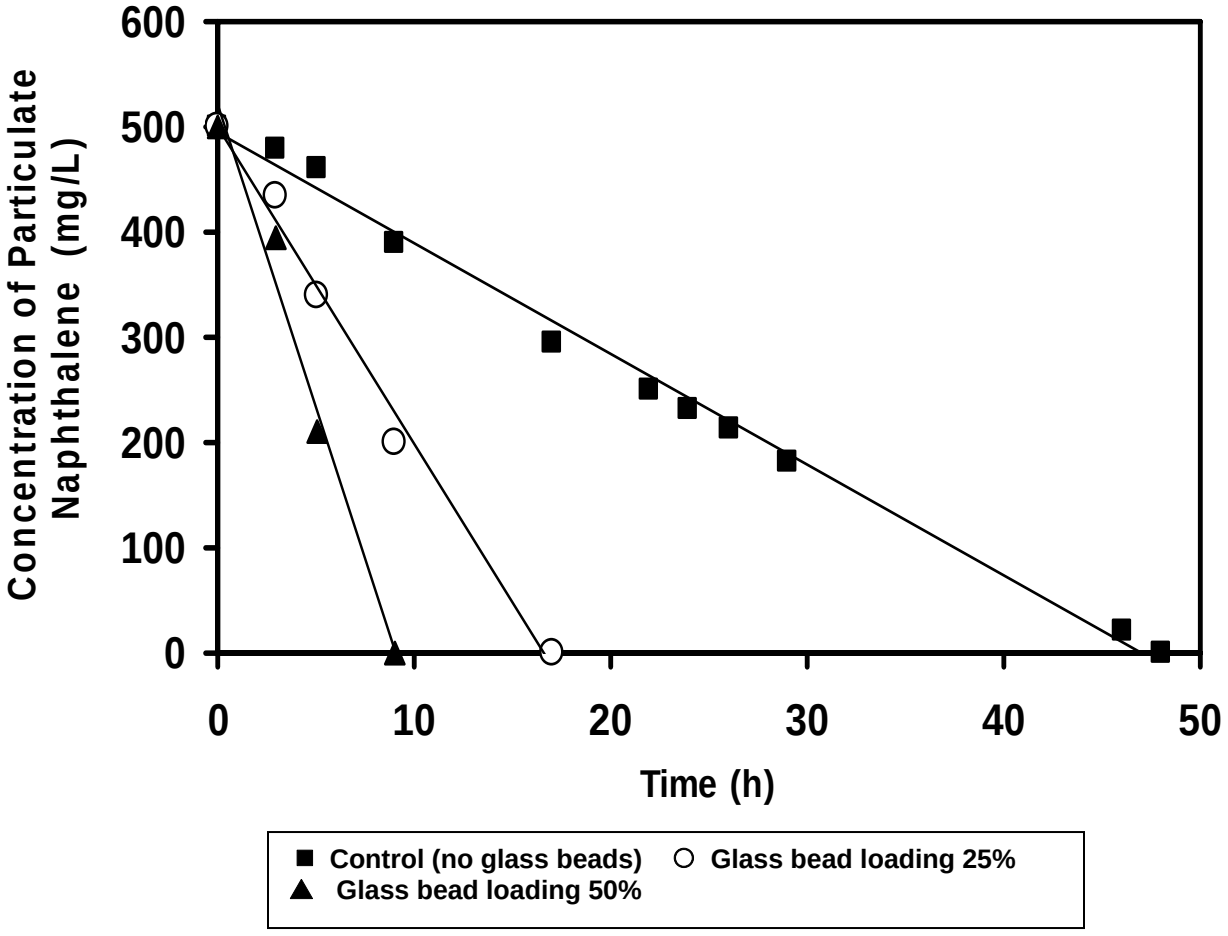

Figure 5.8 Biodegradation of 500 mg/L of particulate naphthalene in conventional roller bioreactor (control) and in the bead mill bioreactors with 25 and 50% loadings of 5 mm glass beads

5.3 2-Methylnaphthalene Mass Transfer

Once the optimum conditions for mass transfer and biodegradation of naphthalene were determined by using the previously discussed experimental variables, efforts were made to apply the optimum mass transfer conditions to a slightly more complex PAH, 2-methylnaphthalene, in the hope that similar mass transfer gains could be achieved. The mass transfer results for 2-methylnaphthalene at optimum conditions is presented in Figure 5.9. The conditions used were 50% loading of 5 mm spherical glass beads.

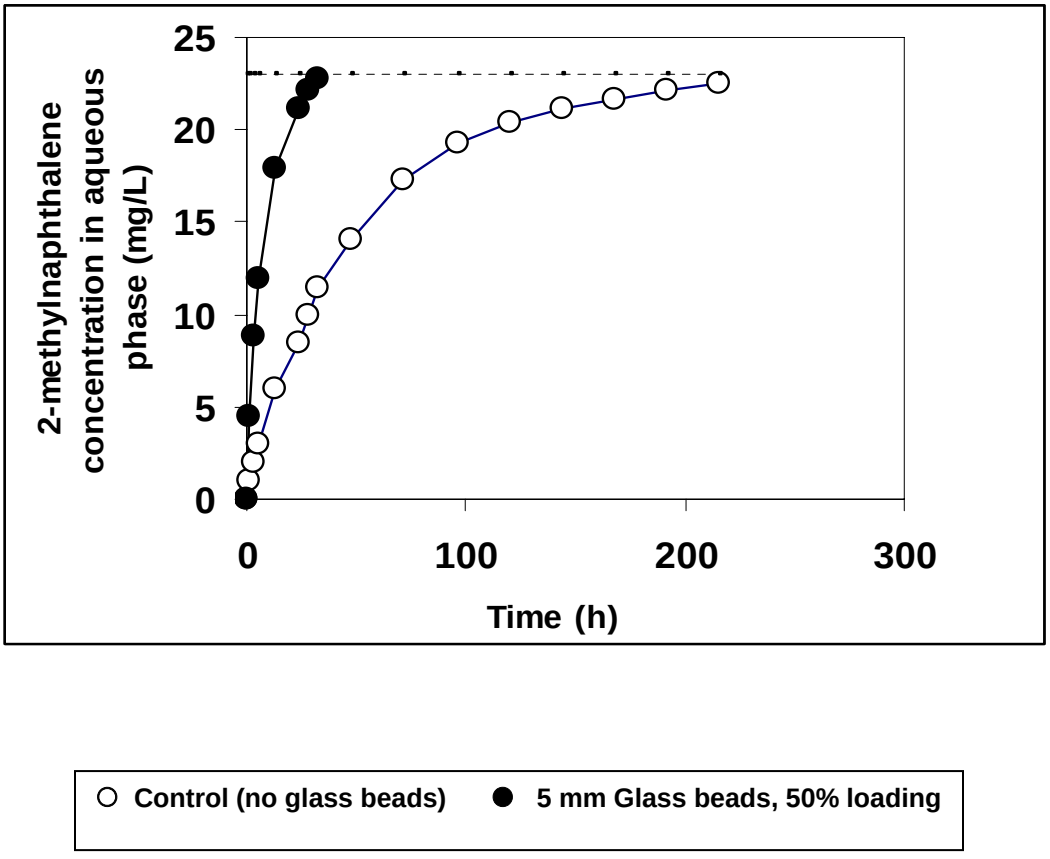

Figure 5.9 Dissolution of 1000 mg/L particulate 2-methylnaphthalene in conventional roller bioreactor and bead mill bioreactor

Clearly, significant gains in mass transfer were observed when applying the optimum mass transfer conditions found in the previous experiments to 2-methylnaphthalene. In our control condition, it took over two hundred hours for 2-methylnaphthalene concentration to reach saturation levels, while in the bead mill bioreactor, saturation concentration is reached in thirty-two hours. The value of mass transfer coefficient calculated for the bead mill and roller bioreactors (control) were 0.12 and 0.02 h^{-1}, respectively. The mass transfer rate of 2-methylnaphthalene was improved about six times when compared to the control condition, while with naphthalene the improvement in mass transfer was around ten-fold. The reasons for less improvement in mass transfer include the lower solubility of 2-methylnaphthalene and its increased hydrophobicity due to the presence of the methyl group. 2-Methylnaphthalene particles also seemed to clump together much easier than naphthalene particles, thereby reducing the effective surface area for mass transfer.

5.4 2-Methylnaphthalene Biodegradation

2-methylnaphthalene was subsequently subjected to the same biodegradation procedures as used for naphthalene at optimum conditions. The results of biodegradation studies with 2-methylnaphthalene are shown in Figure 5.10. As expected the rate of biodegradation in the bead mill bioreactor was significantly faster than that in the conventional roller bioreactor. The bead mill bioreactor showed excellent performance with respect to biodegradation of 2-methylnaphthalene. Compared with a biodegradation rate of 2.7 $mgL^{-1}h^{-1}$ obtained in the conventional roller bioreactor, employment of

the bead mill bioreactor led to an enhanced biodegradation rate of 22.8 $mgL^{-1}h^{-1}$. The biodegradation rate was enhanced nearly eight times, while mass transfer was enhanced six times. It was observed that for naphthalene, close to 100% of the mass transfer gains were reflected in the biodegradation rate, while for 2-methylnaphthalene, over 100% of the mass transfer gains were applied to the degradation rate. It has been shown in the past that biodegradation of 2-methylnaphthalene is possible (Heitkamp and Cerniglia, 1989, Mahajan et al., 1994), however there is no existing literature showing biodegradation rates of 2-methylnaphthalene, so comparison of the biodegradation rate achieved in this work with literature data was not possible.

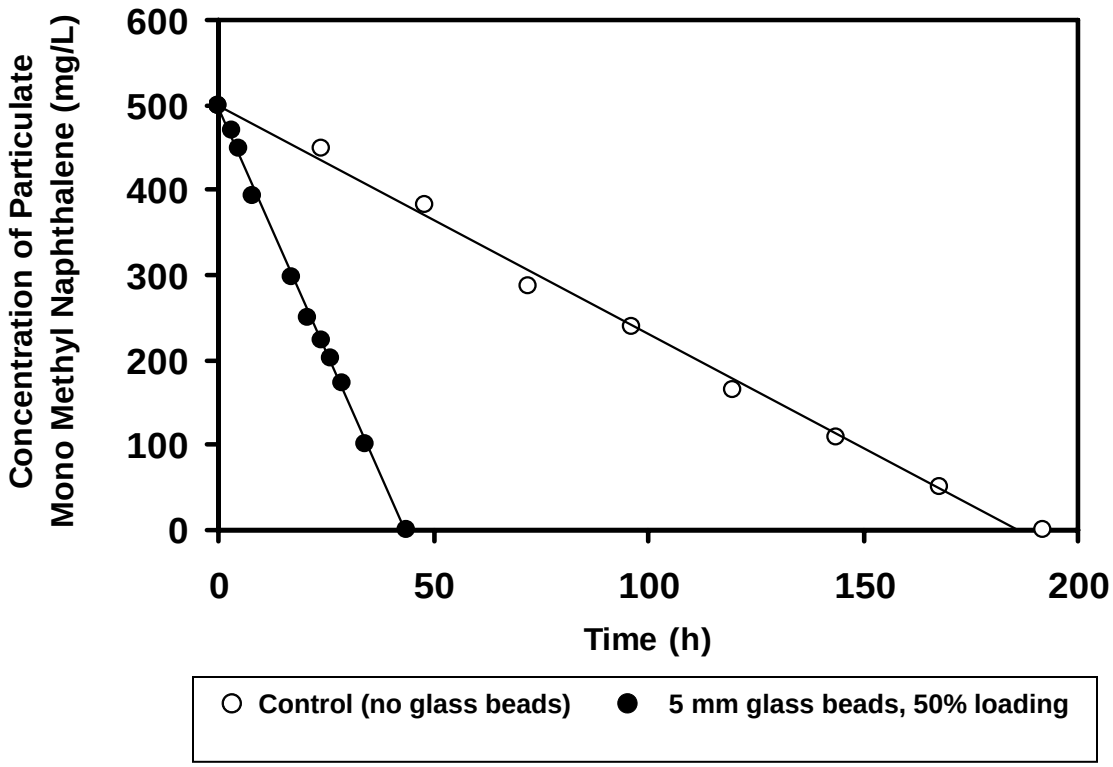

Figure 5.10 Biodegradation of 500 mg/L of particulate mono-methyl-naphthalene in the conventional roller bioreactor (control) and in the bead mill bioreactors

5.5 1,5 Dimethyl Naphthalene Mass Transfer

Mass transfer experiments were undertaken also with 1,5-dimethylnaphthalene (a more complex PAH molecule). The results are summarized in Figure 5.11. As is clearly evident from this figure, this compound is extremely hydrophobic with solubility in the range of 12 mg/L. In the control condition the concentration of 1,5 dimethylnapthalene reached to saturation level in six days, while in the bead mill bioreactor it took only twelve hours. This huge improvement is primarily due to the huge increase in turbulence in the bead mill bioreactor. In the control condition, all of the particles were observed to come together as a large aggregate floating on top of the water, thereby reducing the surface area for mass transfer significantly. In the bead mill, the turbulence prevented the formation of this aggregate and mass transfer proceeded reasonably quickly.

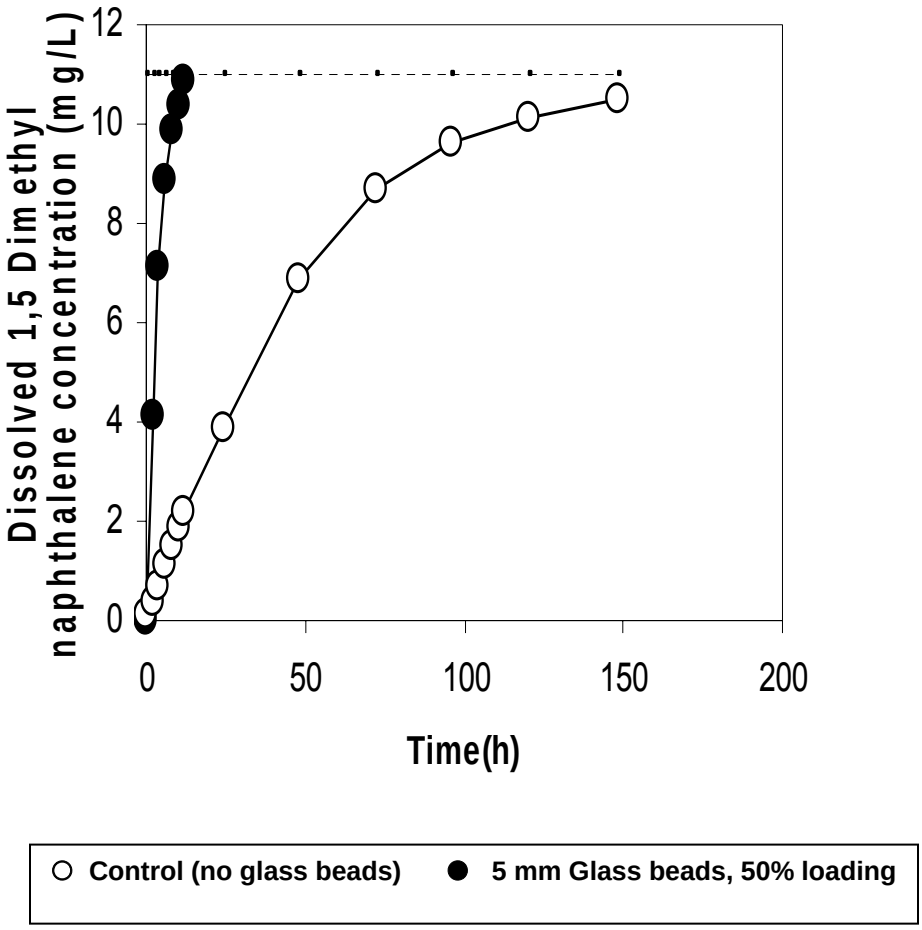

Figure 5.11 Dissolution of 1000 mg particulate 1,5-dimethylnaphthalene in conventional roller bioreactor and bead mill bioreactor

5.6 1,5 Dimethyl Naphthalene Biodegradation

Unfortunately, although 1,5 dimethylnaphthalene has been shown to be amenable to biodegradation by various bacterial species (Dutta et al., 1998), the candidate bacterium used in this work, *Pseudomonas putida*, was unable to degrade the substance. The mass transfer results would indicate great promise for the technology with a suitable bacterial culture.

5.7 Cometabolization of Naphthalene and 2-methylnaphthalene

Experiments were carried out to determine the effects of cometabolization of two PAHs. Both naphthalene and 2-methylnaphthalene were initially present in the system. Figure 5.12 summarizes the experimental data for these biodegradation experiments. The bacteria preferentially used the naphthalene first and then proceeded to degrade the 2-methylnaphthalene at a rate greater than that when grown on 2-methylnaphthalene alone. This result shows some promise, although feedback inhibition would likely limit the effectiveness of this technique for enhancing biodegradation rates.

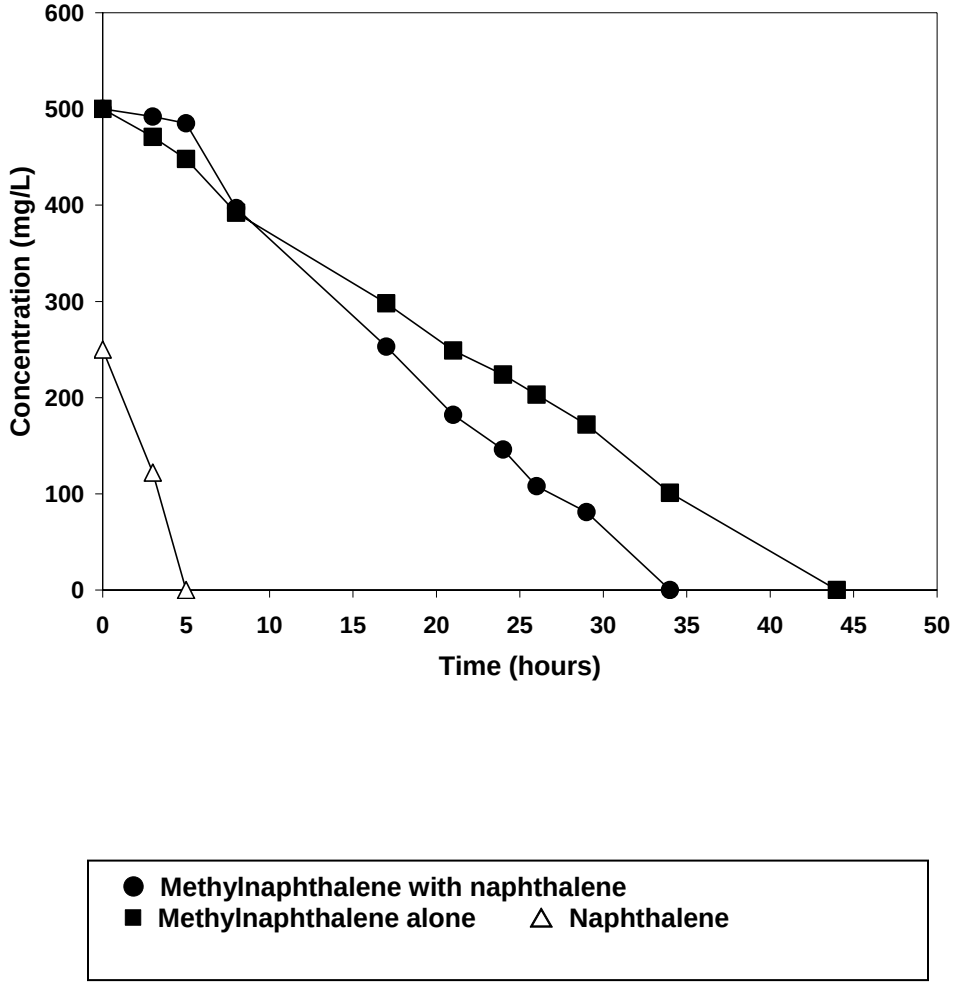

Figure 5.12 Biodegradation of 250 mg/L naphthalene and 500 mg/L 2-methylnaphthalene

5.8 Scale-up Biodegradation Experiments

In order to ascertain the effects of a larger working volume on the biodegradation rate, scale up experiments were undertaken on a larger roller apparatus using two different reactors. The inert particles used in these experiments were glass marbles with a 15 mm diameter. The 15 mm inert particles were chosen based on a series of mass transfer experiments performed by another student. Other than the larger scale, larger inert particles, constant addition of air, and the lack of light in the largest reactor, all variables were kept identical to smaller scale experiments. Scale up was performed to ascertain the possible viability of the technology for large scale treatment of industrial wastes. The rotation speed of the reactors of 50 rpm meant that the larger reactors walls traveled at a greater speed than the smaller reactors due to the increase in radius. The results of the scale up experiments indicate promise for possible industrial applications in the future.

Figures 5.13 and 5.14 demonstrate biodegradation results obtained in a 20 L reactor (8 L working volume) and in a 58 L reactor (23 L working volume) respectively.

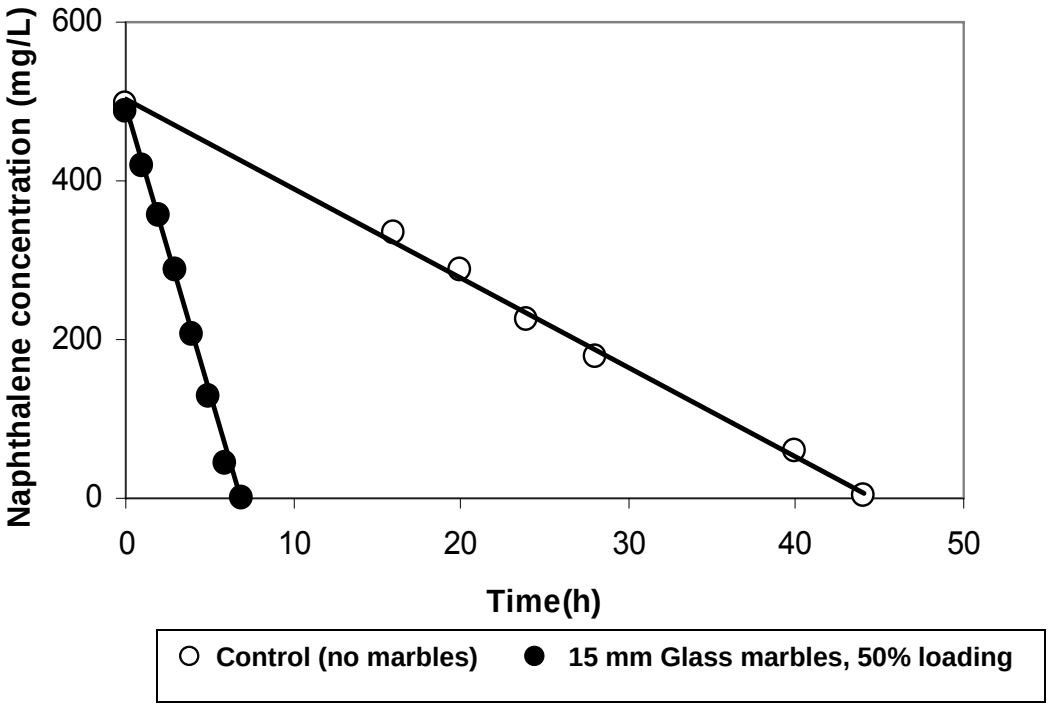

Figure 5.13 Biodegradation in 20 L reactor (8 L working volume)

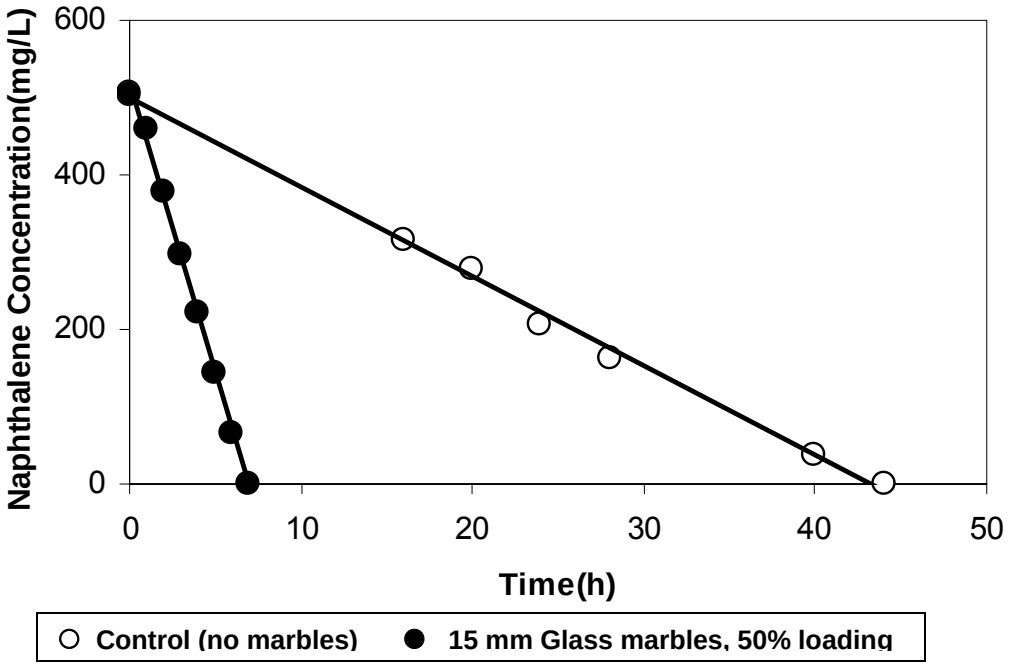

Figure 5.14 Biodegradation in 58 L reactor (23 L working volume)

Clearly demonstrated in Figures 5.13 and 5.14 is that biodegradation proceeds more quickly in the larger vessels. Biodegradation in the intermediate 8L working volume was complete in less than 8 hours and a maximum degradation rate of 72.5 $mgL^{-1}h^{-1}$ was achieved. Biodegradation in the largest 23L working volume was complete in just over 7 hours, with a maximum degradation rate of 74.6 $mgL^{-1}h^{-1}$. As can be seen in Figure 4.4, the largest reactor used was impermeable to light, while the other reactors used allowed light to pass into the reactor. The lack of light in the reactor shows no ill effects on the process and *Pseudomonas putida* is not reported to be sensitive to light conditions. (Selifinova and Eaton, 1996) The 23 L working volume reactor demonstrated a 26% increase in biodegradation speed when compared with the maximum obtained in the 1L working volume. Table 5.1 shows a comparison of the technology developed in this work with other technologies employed to degrade naphthalene. The method developed in this work is shown to be decidedly superior to other systems employing free cells in solution and also superior to much more complex and expensive systems such as the partitioning bioreactor.

Table 5.1 Naphthalene biodegradation rates as reported in various studies

Reference	Microorganism	Physical state of the cells	Biodegradation rate ($mgL^{-1}h^{-1}$)
(Manohar and Karegouda, 1998)	*Pseudomonas* NGK1	Freely suspended cells	33.4-44.5
(Wang et al., 2001)	*Flavobacterium* sp.	Freely suspended cells	0.7-2.5
(Punt et al., 2002)	*Sphingomonas arimaticivorans*	Freely suspended cells	33
(Manohar and Karegouda, 1998)	*Pseudomonas* NGK1	Immobilized in Ca-alginate	21.4-38.1
(Manohar and Karegouda, 1998)	*Pseudomonas* NGK1	Immobilized in agar	40-53.4
(Manohar and Karegouda, 1998)	*Pseudomonas* NGK1	Immobilized in poly foam	67
(Daugulis et al., 2001)	*Sphingomonas arimaticivorans*	Free Cells	119
Present work	*Pseudomonas putida* (ATCC 17484)	Freely suspended cells	148

5.9 BIOREMEDIATION PRODUCTS

As the PAHs were clearly being degraded by the candidate bacteria, the question of what the end products of that degradation were became pertinent. Figure 5.16 presents HPLC chromatograms demonstrating what is happening during the degradation process. In the initial sample, there is nothing but 500 mg/L of naphthalene in the solution. As the biodegradation progresses, we see the naphthalene concentration dropping steadily and the accumulation of an end product with a retention time of around 0.63 minutes. This end product was not successfully identified, although numerous attempts were made to do so. Previous work done by Purwaningsih (2002) identified the end product of this degradation process as catechol, with a retention time of around 0.88 minutes. She found that catechol provided feedback inhibition to the bacteria and that the maximum amount of naphthalene she could degrade was 750 mg/L. The end product in our case is metabolized by the bacteria slowly once all the initial naphthalene is gone, and does not seem to provide feedback inhibition. The reasons for a differing end product may have to do with the increased turbulence in the reactor, ensuring bacteria ample oxygen at any given time. At the point where all the naphthalene is metabolized, there is approximately 60 mg/L of this unknown substance in solution. To ensure that this unknown end product is not more toxic than naphthalene, toxicity testing using brine shrimp was undertaken.

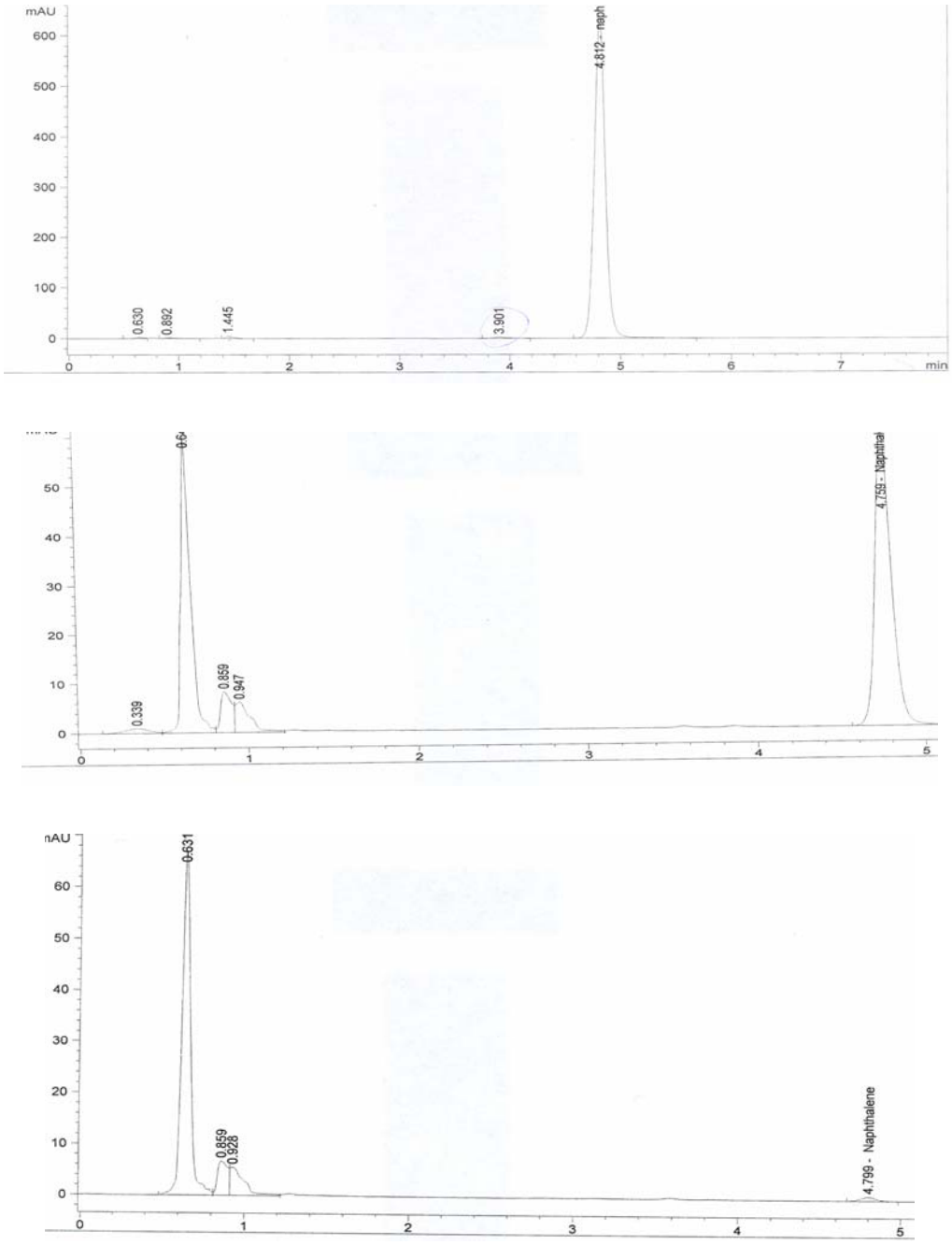

Figure 5.16: HPLC chromatograms of the biodegradation progress. Top – initial reading, middle – intermediate reading, bottom – final reading.

5.10 TOXICITY RESULTS

It was desired to ascertain the effect that bioremediation had on the toxicity of the reactor contents. Experiments were set up and carried out following the procedure outlined in Chapter 4. The final effluent of the 23L reactor after 12 hours of biodegradation was used as the final biodegradation product. The initial samples were saturated naphthalene solution, and the control was distilled water. Table 5.2 shows the data from toxicity testing. All numbers in the table refer to number of viable shrimp present at a given time.

Table 5.2: Toxicity data

Time(h)	Control 1	Control 2	Initial 1	Initial 2	Final 1	Final 2
0	13	39	22	31	25	29
0.50	13	38	7	9	24	28
1	13	38	2	5	24	27
2	12	38	0	0	22	27

From the toxicity data it is clear that the initial, saturated naphthalene solution is lethal to the organisms. After only two hours, all viable organisms exposed to the saturated naphthalene solution are dead. This is compared to the control where over 96% remain alive after the two hours and the final biodegradation product in which over 90% remain alive after two hours. The final effluent is much less toxic than the saturated naphthalene solution which was subjected to biodegradation. The final effluent compares favourably with the control.

CHAPTER 6 CONCLUSIONS AND RECOMMENDATIONS

6.1 Conclusions

The following conclusions can be made from the present work.

1. The addition of inert particles to the reactor had the desired effect on the system, increasing the mass transfer rate. The use of 50% loading of 5 mm glass beads increased the volumetric mass transfer coefficient by a factor of ten to a maximum value of 0.71 h^{-1} at an initial naphthalene loading of 1000 mg/L.
2. From a mass transfer stand point, spherical glass beads were found to be more effective than cylindrical Raschig rings. The increase in the diameter of glass beads improved the extent of mass transfer.
3. Mass transfer rates were found to increase with increased levels of PAH loading. These increases were much more pronounced in the presence of glass beads (Bead Mill Bioreactor) as opposed to the control roller bioreactor. This further confirms the effectiveness of glass beads as a mass transfer aid.
4. The biodegradation rate of naphthalene in the bead mill bioreactor (118.4 $mgL^{-1}h^{-1}$) was eleven-fold faster than that in the control bioreactor (10.6 $mgL^{-1}h^{-1}$).
5. Application of bead mill bioreactor enhanced the biodegradation rate of 2-methylnaphthalene by a factor of 8. While a biodegradation rate of 2.7

$mgL^{-1}h^{-1}$ was obtained in the conventional roller bioreactor, in the bead mill bioreactor the observed rate was 22.8 $mgL^{-1}h^{-1}$.

6. The biodegradation rate of 2-methylnaphthalene increased upon cometabolization with a small amount of naphthalene. Under these conditions 500mg/L of 2-methylnaphthalene was completely degraded in 34 hours, giving a degradation rate of 29.4 $mgL^{-1}h^{-1}$. Cometabolization leads to an improvement of over 25 % in the rate of degradation of 2-methylnaphthalene.
7. The candidate bacterium used in this study (*Pseudomonas putida* ATCC 17484) was not able to metabolize 1-5 dimethylnaphthalene, or cometabolize it in the presence of naphthalene or 2-methylnaphthalene.
8. Improved biodegradation rates were observed in the semi-pilot scale bioreactors. A 23 times increase in the bioreactor working volume coupled with a 3-fold increase for inert particle diameter at the same rotation speed of 50 rpm led to a biodegradation rate of 148.8 $mgL^{-1}h^{-1}$. This represents a 26% increase in the biodegradation rate when compared with the original, small-scaled Bead Mill Bioreactor. This demonstrates that this technology has great potential for industrial applications.
9. The final broth of the naphthalene bioremediation process contained an unknown compound, but the toxicity of this substance was found to be negligible to brine shrimp larvae cells.

6.2 Recommendations

The following recommendations should be considered in future studies:

1. The use of baffles within the developed bead mill bioreactor may further improve the extent of mass transfer. The addition of baffles to the system may also decrease the loading of the beads needed for optimum mass transfer and thereby increase the working volume available for bioremediation.
2. A range of different bacterial species may be utilized in order to expand the application of the bead mill bioreactor for treatment of a variety of PAHs. A mixed culture may be able to degrade PAHs more quickly and at higher initial concentrations. Because feedback inhibition is found to be a problem at higher PAH concentrations, a bacterial species that preferentially metabolized the inhibitory products should enhance the degradation performance of this bioreactor.
3. Additional scale up studies should be undertaken to determine the effects of larger scale treatment for possible industrial applications.
4. Investigation of more porous inert particles should be undertaken. This may encourage the formation of the biofilm on the particles, leading to increased biomass hold-up and faster biodegradation rates. Additionally, the establishment of biofilm in the system could facilitate the operation of the bioreactor continuously. The porous particles must be heavy enough to have sufficient impact on mass transfer, however, as the data obtained for Raschig rings clearly demonstrates.

5. The effects of using a mixture of beads of different sizes within the reactor should be investigated. This should lead to better grinding of particulate matter if that is of concern and also may increase solid-liquid mass transfer rates.
6. The remediation of contaminated soils should be investigated as the crushing action of the beads should be beneficial in remediation of fractile particles.
7. The effects of diameter, both of the reactor itself and of the inert particles, should be investigated further. A model of these effects would be invaluable.
8. The effects of inert particles on oxygen mass transfer would be a very useful thing to study in the future.

REFERENCES

Alexander, M. (1999) Biodegradation and Bioremediation, 2nd ed., Academic Press, Toronto.

Bailey, J. E. and Ollis, P. F., (1977) Biochemical Engineering Fundamentals., McGraw-Hill, New York.

Black, J.G. (1996) *Microbiology. Principles and Applications.* Third Edition. Prentice Hall. Upper Saddle River, New Jersey. pp. 136-140, 151-153.

Bouchez, M., Blanchet, D. and Vandecasteele, J.P., (1995) Degradation of Polycyclic Aromatic Hydrocarbons by Pure Strains and Defined Strain Associations: Inhibition Phenomena and Cometabolism, *Appl. Microbiol. Biotechol*., 43: 156-164

Brinkmann D, Rohrs J. and Schugerl K. (1998) Bioremediation of diesel fuel contaminated soil in a rotating bioreactor: Influence of oxygen saturation. Chem Eng Technol 21: 168-172.

Canadian Environmental Protection Act, (1994) Priority Substances List Assessment Report, Polycyclic Aromatic Hydrocarbons: 6

Chiou, C.T., S.E. and McGroddy, D.E. Kile (1998) Partitioning characteristics of polycyclic aromatic hydrocarbons on soils and sediments, *Environ. Sci. Technol.*, 32(2):2769-2775.

da Silva M, Cerniglia CE, Pothuluri JV, Canhos VP and Espoisto E, (2003) Screening filamentous fungi isolated from estuarine sediments for ability to oxidize polycyclic aromatic hydrocarbons. *World J Microbiol Biotechnol* 19:399–405

Daugulis AJ and Janikowski TB, (2002) Scale-up performance of a partitioning bioreactor for the degradation of polyaromatic hydrocarbons by *Sphingomonas aromaticivorans*. *Biotechnol Lett* 24:591–594.

Dutta, T. K., Selifonov S. A., and Gunsalus, I. C.**.** (1998) Oxidation of methyl-substituted naphthalenes: pathways in a versatile *Sphingomonas paucimobilis* strain. Appl. Environ. Microbiol. 64:1884-1889

Gray MR, Banerjee DK, Fedorak PM, Hashimoto A, Masliyah JH, and Pickard MA. (1994) Biological remediation of anthracene contaminated soil in rotating bioreactors. Appl Microbiol Biotechnol 40: 933-940.

Haldane, J.B.S., (1930) Enzymes. Longmans, London.

Heitkamp, M. A., and Cerniglia C. E.. (1989) Polycyclic aromatic hydrocarbon degradation by a *Mycobacterium* sp. in microcosms containing sediment and water from a pristine ecosystem. Appl. Environ. Microbiol. 55:1968–1973.

Hill GA. and Robinson CW (1975) Substrate inhibition kinetics: phenol degradation by *Pseudomonas putida*. Biotechnol Bioeng 17: 1599–1615

Hill, G.A., Milne, B. J., and Nawrocki, P.A., (1996) Cometabolic degradation of 4-chlorophenol by *Alcaligenes eutrophus, Appl. Microbiol. Biotechnol*., 46: 163-168.

Horvarth, R.S., (1972) Microbial cometabolism and the degradation of organic compounds in Nature, *Bacteriological Rev*. 36: 146-155.

Kanaly RA and Haryama S (2000) Biodegradation of high molecular weight polycyclic aromatic hydrocarbons by bacteria. J Bacteriol. 182: 2059-2067.

LaBranche D.F, and Collins M.R.,(1996) "Stripping volatile organic compounds and petroleum hydrocarbons from water," Water Environment Research, Vol. 68(3), pp. 348-358,

Langworthy DE, Stapleton RD, Sayler GS and Findlay RH (2002) Lipid analysis of the response of a sedimentary microbial community to polycyclic aromatic hydrocarbons. Microbiol Ecol. 43:189-198.

Mahajan MC, Phale PS and Vaidyanathan CS. (1994) Evidence for the involvement of multiple pathways in the biodegradation of 1- and 2-methylnaphthalene by *Pseudomonas putida* CSV86. Arch Microbiol. 1994;161(5):425-433.

Maier, R.M (2000) Bioavailability and Its Importance to Bioremediation, in Bioremediation, ed. By James, V.J., Kluwer Academic Publisher, Boston.

Manohar S, Kim CK and Karegoudar TB. (2001) Enhanced degradation rate of naphthalene by immobilization of *Pseudomonas* sp Strain NGK1 in polyurethane foam. *Appl Microbiol Biotechnol* 55:311–316

Manohar S and Karegoudar TB. (1998) Degradation of naphthalene by cells of *Pseudomonas* sp strain NGK 1 immobilized in alginate, agar and polyacrylamide. *Appl Microbiol Biotechnol* 49:785–792

Marr, L. C., Kirchstetter T. W., Harley R. A., Miguel A. H, Hering S. V., and Hammond S. K.. (1999) Characterization of polycyclic aromatic hydrocarbons in motor vehicle fuels and exhaust emissions. Environ. Sci. Technol. 33:3091-3099.

McMillen, S.J., Magaw R. I., and Carovillano R.L., (2001) "Risk-Based Decision-Making for Assessing Petroleum Impacts at Exploration and Production Sites," U.S. Department of Energy and Petroleum Environmental Research Forum, October

Monod, J. (1942) Recherches sur la Croissainces des Cultures Bacteriennes, Herman and Cie, Paris.

Mulder H, Breure AM, van Honschooten D, Grotenhuis JTC, van Andel JG and Rulkens WH. (1998) Effect of biofilm formation by *Pseudomonas* 8909N on the bioavailability of solid naphthalene. Appl Microbiol Biotechnol 50: 277-283.

OECD, 1999, OECD Environmental Data: Compendium (1999) OECD Publications, Paris

Perera F, Hemminki K and Jedrychowski W, et al.(2002) In utero DNA damage from environmental pollution is associated with somatic gene mutation in newborns. Cancer Epidemiol Biomarkers Prev;11:1134–1137

Phillips, D. H**.** (1983) Fifty years of benzo[*a*]pyrene. Nature 303**:**468-472.

Prabhu Y and Phale PS (2003) Biodegradation of phenanthrene by *Pseudomonas* sp. Strain PP2: novel metabolic pathway, role of biosurfactant and cell surface hydrophobicity in hydrocarbon assimilation. Appl Microbiol Biotechnol. 61: 342-351.

Punt M, Janikowski TB, Velicogna D and Daugulis AJ, (2002) Use of a two-phase partitioning bioreactor for degrading polycyclic aromatic hydrocarbons by a *Sphingomonas* sp. *Appl Microbiol Biotechnol* 59:368–376

Purwaningsih, I., (2002) Mass Transfer and Biodegradation of Solid Polycyclic Aromatic Hydrocarbon (PAH) Particles in Bioreactors, PhD. Thesis, University of Saskatchewan.

Purwaningsih, I., Hill G.A and Headley J.V., (2004) Mass transfer and bioremediation of naphthalene particles in a roller bioreactor. Water Research, 38, 2027–2034.

Selifonova, O. V., and Eaton R.W. 1996. Use of *ibp-lux* fusion to study regulation of the isopropylbenzene catabolism operon of *Pseudomonas putida* RE204 and to detect hydrophobic pollutants in the environment. Appl. Environ. Microbiol. 62**:**778-783

Sims, R.C., and Overcash, M. R., (1983) Fate of polycyclic aromatic compounds in soil-plant systems, *Residue Rev*., 88: 1-68.

Singh, N. and Hill, G.A., (1987) Air stripping effects on cell growth with volatile substrates, *Biotech. Bioeng*., 30:521-527.

Sutherland, J. B. (1992) Detoxification of polycyclic aromatic hydrocarbons by fungi. J. Ind. Microbiol. 9**:**53-62[Medline].

Tarighian, A., (1999) Cometabolic biodegradation of three pulp and paper wastewater components, M. Sc. Thesis, University of Saskatchewan.

Thomas, R. G., (1982) Volatilization from Water, In: Handbook of Chemical Property Estimation Methods, American Chemical Society, Washington, D.C.

Toussaint, M.W., Shedd T.R., Van der Schalie W.H, and G.R. Leather. (1995) A comparison of standard acute toxicity tests with rapid-screening toxicity tests. Environ. Toxicol. Chem. 14:907-915

Twiss, M.R., Granier L., Lafrance P., and Campbell P.G. C**.** (1999) Bioaccumulation of 2,2',5,5'-tetrachlorobiphenyl and pyrene by picoplankton (*Synechococcus leopoliensis*, Cyanophyceae): influence of variable humic acid concentrations and pH. Environ. Toxicol. Chem. 18**:**2063-2069.

Van't Riet, K and Trampe, J., (1991) Basic Bioreactor Design, M. Dekker, New York.

Volkering F, Breure AM, Sterkenburg A and van Andel JG. (1992) Microbial degradation of polycyclic aromatic hydrocarbons: effect of substrate availability on bacterial growth kinetics. Appl Microbiol Biotechnol 36: 548-552.

Volkering, F., Breure, A. M and van Andel, J.G., (1993) Effect of Microorganisms on the Bioavailability and Biodegradation of Crystalline Naphthelene, *Appl. Microbiol. Biotechnol*., 40; 535-540.

Wang, X., Yu X., and Bartha R**.** (1990) Effect of bioremediation on polycyclic aromatic hydrocarbon residues in soil. Environ. Sci. Technol. 24**:**1086-1089.
World Health Organization, 1983, Evaluation of The Carcinogenic Risk of Chemicals to Human-Polycyclic Aromatic Hydrocarbons. Part 1: Chemical, Environmental and Experimental Data, 32, I.A.R.C, Lyons, France.

Wang, X and Brusseau, M. J.,(1993) Solubilization of some low-polarity organic compounds by hydroxypropyl-B-cyclodextrin, *Environ. Sci. Technol*. 27:2823-2825.

Wang S and Vipulanandan C,(2001). Biodegradation of naphthalene contaminated soils in slurry bioreactors. *J Environ Eng* 748–754

Wilson, S. and Jones K.. (1993) Bioremediation of soil contaminated with polynuclear aromatic hydrocarbons (PAHs): A review, Environmental Pollution, 81: 229-249.

Wilson AS, Davis CD, Williams DP, Buckpitt AR, Pirmohamed M, M and Park BK: (1996) Characterisation of the toxic metabolite(s) of naphthalene. Toxicology 114, 233-234

APPENDICES

Appendix A1: Calibration of biomass dry weight

The procedure for calculating biomass dry weight is outlined in section 4.3.3. Four different samples were used and the correlation obtained is excellent. The curve is shown in Figure A1.

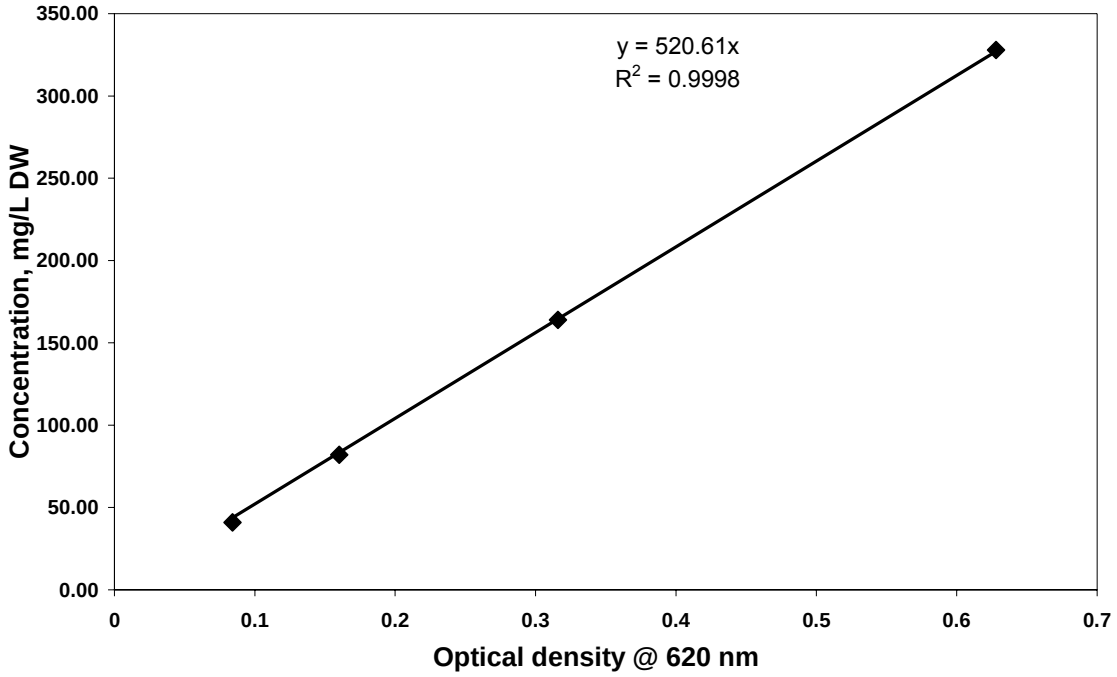

Figure A1: Calibration curve for biomass dry weight

Appendix A2: HPLC calibration curve for naphthalene

Dissolved and total naphthalene concentrations were measured using HPLC. Particles were dissolved in a 2:1 ratio of ethanol: water as per the procedure outlined in Section 4.3.4. The Y-axis shows the chromatogram response and the X-axis naphthalene concentration. The relation is linear and is shown in Figure A2. The residence time in the column was 4.7 minutes.

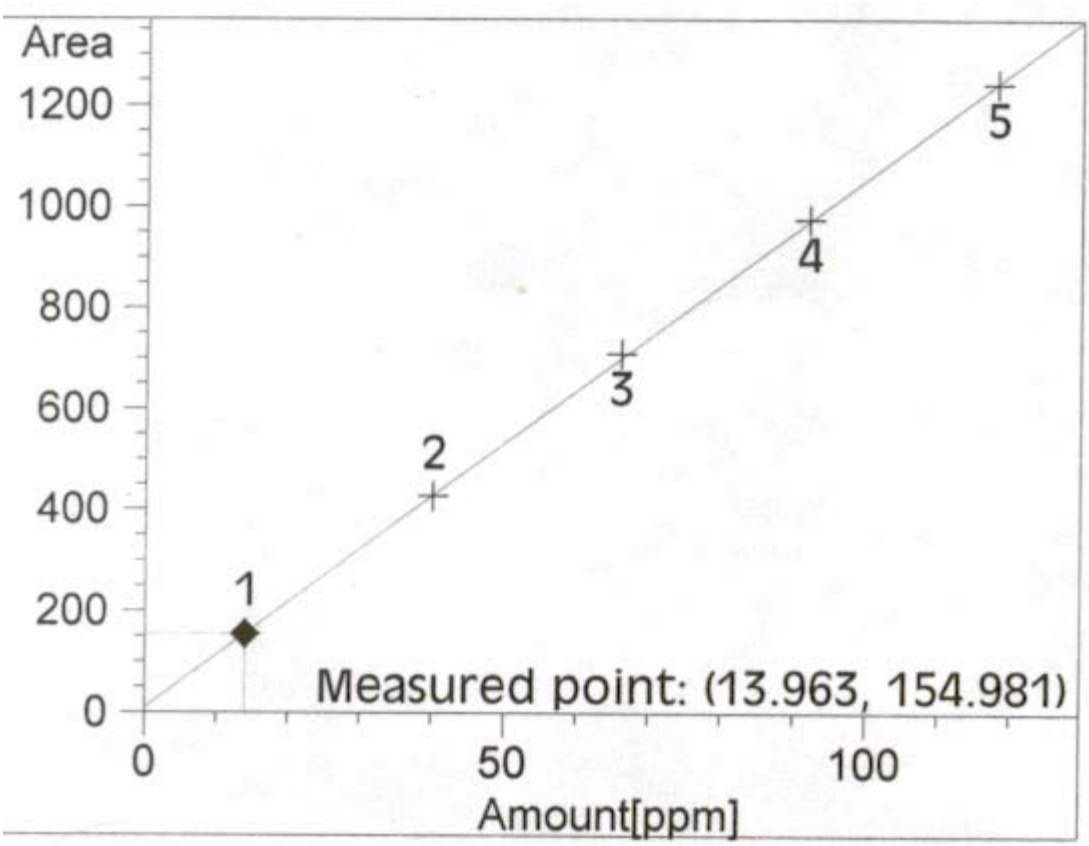

Figure A2: HPLC calibration curve for naphthalene

Appendix A3: HPLC calibration curve for 2-methylnaphthalene

Dissolved and total 2-methylnaphthalene concentrations were measured using HPLC. Particles were dissolved in a 2:1 ratio of ethanol: water as per the procedure outlined in Section 4.3.4. The Y-axis shows the chromatogram response and the X-axis naphthalene concentration. The relation is linear and is shown in Figure A3. Residence time in the column was 7.6 minutes.

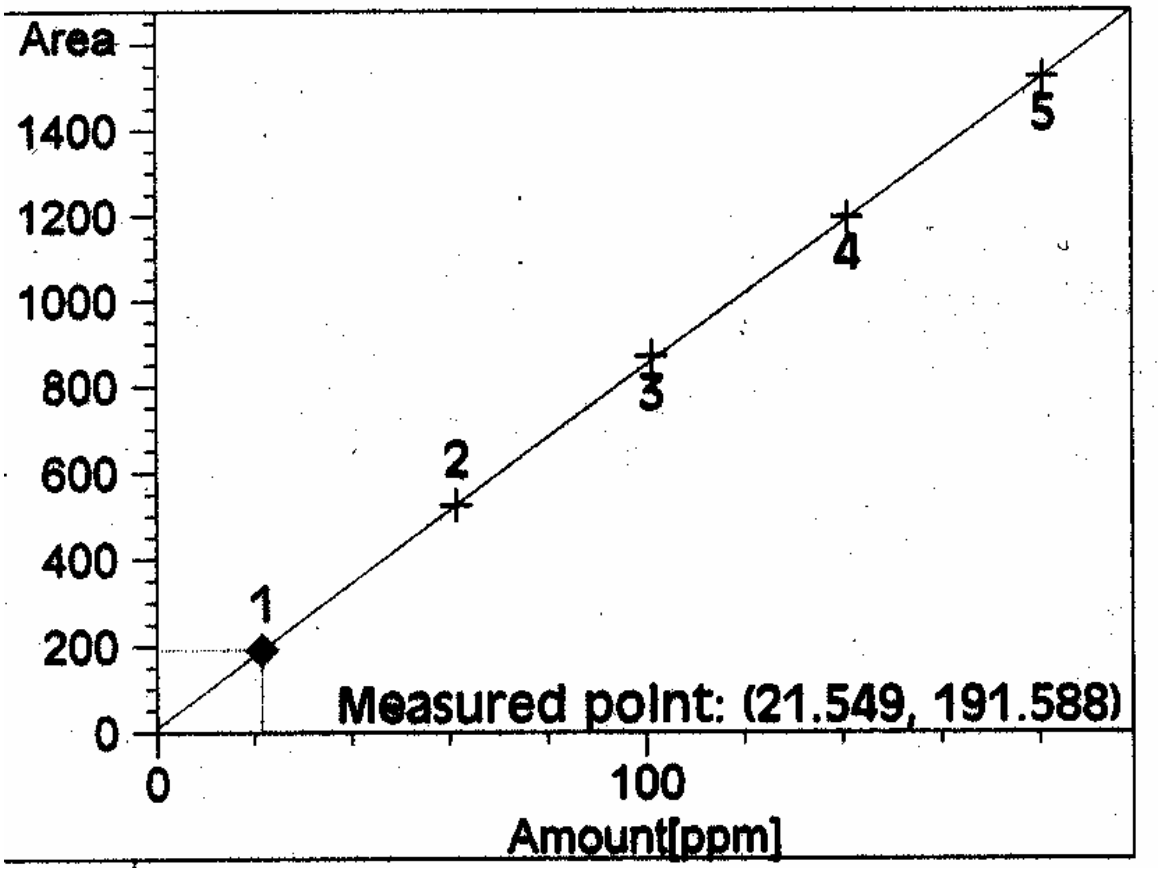

Figure A3: HPLC calibration curve for 2-methylnaphthalene

Appendix A4: HPLC calibration curve for 1,5-dimethylnaphthalene

Dissolved and total 1,5 dimethylnaphthalene concentrations were measured using HPLC. Particles were dissolved in a 2:1 ratio of ethanol: water as per the procedure outlined in Section 4.3.4. The Y-axis shows the chromatogram response and the X-axis naphthalene concentration. The relation is linear and is shown in Figure A3. The residence time was 10.9 minutes.

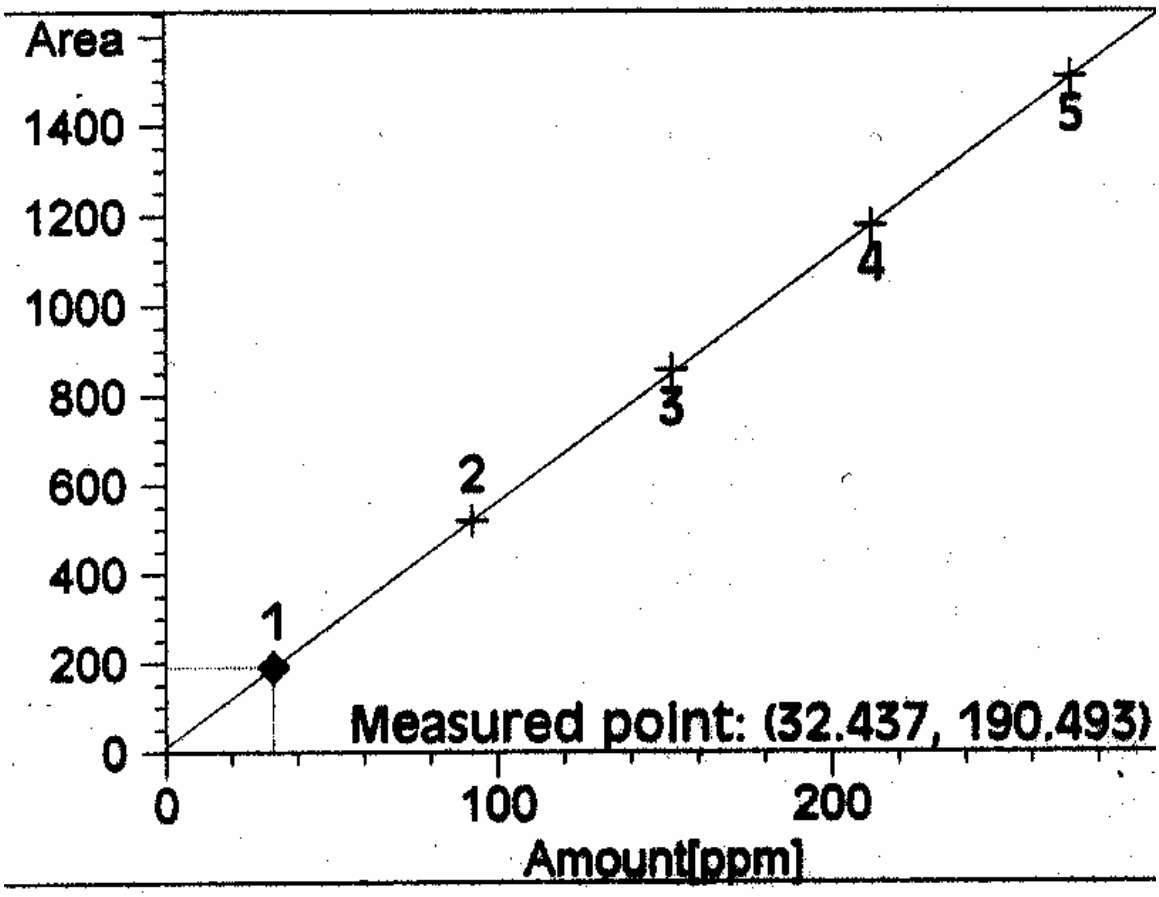

Figure A4: HPLC calibration curve for 1,5-dimethylnaphthalene

Appendix B: Experimental Data

Table B1: Mass transfer comparison with 3mm beads in various loadings with solid naphthalene present at 1000mg/L

Time(h)	25%	50%	10%	0%	75%
0	0	0	0	0	0
0.5	5.8	13.9	3.5	0.9	14.5
1	9.9	21.9	6.8	1.9	22.3
2.5	18.3	27	11.3	4.2	27.4
4	25	31	15	6.2	
8	31	32	24	13.3	

Table B2: Mass transfer comparison with 3mm beads in various loadings with solid naphthalene present at 500 mg/L

Time(h)	Control	10%	25%	50%
0	0	0	0	0
0.5	0.6	3.1	5.5	6.4
1	1.1	5.8	8.9	12.3
2.5	3.5	9.3	15.7	20.1
4	5.8	13	22.3	27.3
8	11.1	18.7	25.6	31

Table B3: Mass transfer comparison with 3mm beads in various loadings with solid naphthalene present at 5000 mg/L

Time (h)	10%	25%	50%	Time(h)	Control
0	0	0	0	0	0
0.25	5	11	18	0.5	3.4
0.5	8.3	16.3	23.5	1	6.1
0.75	12.3	22.7	27.9	2.5	9.6
1	17.2	26.4	30.2	4	13.6
1.5	23.9	30.7	32.1	8	19.7
2.5	27.2	32.1	32.2		

Table B4: Mass transfer comparison with 3mm beads in various loadings with solid naphthalene present at 10000 mg/L

Time	10%	25%	50%	Time(h)	Control
0	0	0	0	0	0
0.25	5.5	12.1	19	0.5	3.7
0.5	9.2	17.9	24.9	1	6.4
0.75	13.6	23.9	30.2	2.5	9.8
1	18.9	28.7	31.2	4	13.9
1.5	26.4	31.2	32.1	8	20.4
2.5	30.1	32.1	32.2		

Table B5: Mass transfer comparison with various mass transfer aids at 50% loading. Naphthalene present at 1000mg/L

Time (h)	1mm	3mm	5mm	Raschig	control
0	0	0	0	0	0
0.5	9.2	13.9	15.9	7.8	0.9
1	16.3	21.9	23.1	14.1	1.9
2.5	23.2	27	31	20.9	4.2
4	28.7	31	32	24.9	6.2

Table B6: Biodegradation comparison of 3mm beads at various loadings with control. Initial naphthalene concentration 500mg/L.

Time (h)	Control	50%	25%
0	500	500	500
3	480	395	435
5	460	210	340
9	390	0	200
17	296		0
22	251		
24	231		
26	214		
29	182		
46	22		
48	0		

Table B7: Biodegradation comparison of 5mm beads at various loadings with control. Initial naphthalene concentration 500mg/L.

Time (h)	Control	50%	25%
0	500	500	500
3	480	358	424
5	460	198	329
9	390	0	178
17	296		0
22	251		
24	231		
26	214		
29	182		
46	22		
48	0		

Table B8: Mass transfer control data for 2-methylnaphthalene (1000mg/L)

Time(days)	Conc. (mg/L)
0	0
1	8
2	14
3	17.3
4	19.3
5	20.4
6	21.1
7	21.7
8	22.2
9	22.5

Table B9: Mass transfer optimum data for 2-methylnaphthalene. (50% loading 5mm glass beads, 1000mg/L)

Time(hours)	Conc. (mg/L)
0	0
1	4.5
3	8.8
5	11.9
13	17.9
24	21.2
28	22.2
32	22.8

Table B10: Biodegradation and Cometabolization data for 2-methylnaphthalene at optimum mass transfer conditions

Time (h)	M-nap alone	M-nap w nap	Nap
0	500	500	250
3	471	492	122
5	448	485	0
8	392	397	
17	298	253	
21	249	182	
24	224	146	
26	203	108	
29	172	81	
34	101	0	
44	0		

Table B11: Mass transfer data for 1,5-dimethylnaphthalene at optimum mass transfer conditions and control

Time(hours)	Optimum	Control
0	0	0.1
2	4.1	0.4
4	7.1	0.7
6	8.9	1.1
8	9.9	1.5
10	10.4	1.9
12	10.9	2.2
24		3.9
48		6.9
72		8.7
96		9.6
120		10.1
148		10.5

Table B12: Scale-up biodegradation data for 20L reactor. Marbles occupied 50% of working volume.

Time (h)	Control	Marbles
0	497	493.0
1		419.3
2		357.5
3		286.0
4		207.5
5		128.5
6		42.8
7		1.3
8		
9		
10		
16	333	
20	289	
24	226	
28	179	
40	58	
44	2	

Table B13: Scale-up biodegradation data for 53L reactor. Marbles occupied 50% of working volume.

Time(h)	Control	Marbles
0	505	502
1		459
2		379
3		297
4		221
5		142.5
6		65
7		0
8		
9		
10		
16	317	
20	278	
24	207	
28	161	
40	39	
44	0	